

AD-A124 705

DEPTH-RESOLVED CATHODOLUMINESCENCE STUDY OF ANNEALED
SILICON IMPLANTED GA..(U) AIR FORCE INST OF TECH
WRIGHT-PATTERSON AFB OH SCHOOL OF ENGI... J R CAVINS

1/1

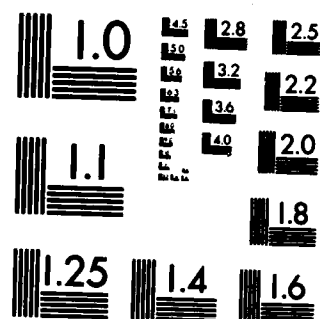
UNCLASSIFIED

DEC 82 AFIT/GEP/PH/82D-2

F/G 20/12

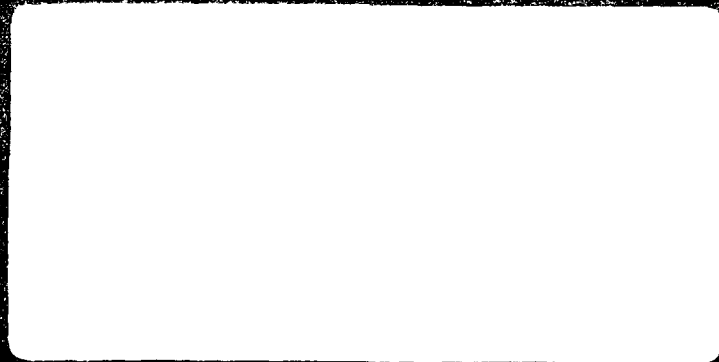
NL

END
DATE
FILMED
FBI
DTIC



MICROCOPY RESOLUTION TEST CHART
NATIONAL BUREAU OF STANDARDS-1963-A

ADA 124705



AFIT/GEP/PH/82D-2

DEPTH-RESOLVED CATHODOLUMINESCENCE
STUDY OF ANNEALED SILICON
IMPLANTED GALLIUM ARSENIDE

THESIS

AFIT/GEP/PH/82D-2 Jeffrey R. Cavins
Captain USAF

DTIC
ELECTE
FEB 22 1983
A

Approved for public release; distribution unlimited.

DEPTH-RESOLVED CATHODOLUMINESCENCE STUDY
OF ANNEALED SILICON IMPLANTED
GALLIUM ARSENIDE

THESIS

Presented to the Faculty of the School of Engineering
of the Air Force Institute of Technology
Air University
in Partial Fulfillment of the
Requirements for the Degree of
Master of Science

by

JEFFREY R. CAVINS
Captain USAF

Graduate Engineering Physics
December 1982

Availability For	
STANDARD	<input checked="checked" type="checkbox"/>
RESTRICTED	<input type="checkbox"/>
UNCLASSIFIED	<input type="checkbox"/>
Classification	
By	
Distribution/	
Availability Codes	
Dist	avail and/or Special
A	



Approved for public release; unlimited distribution.

Preface

The completion of this thesis would not have been possible without the assistance of several individuals. Among them I would like to thank Dr. Robert L. Hengehold, my thesis advisor, for his advice and guidance throughout the work on this thesis. I would also like to thank Ron Gabriel, George Gergal, and Don Ellworth of the AFIT Physics Laboratory for their valuable technical assistance. My thanks also go to AFWAL/AADR, Wright-Patterson AFB, Ohio for providing the samples and the facilities for their preparation. Finally, I would like to thank my wife, Deborah, for exhibiting such patience and understanding during the past 18 months.

Jeffrey R. Cavins

Contents

	<u>Page</u>
Preface.....	ii
List of Figures.....	v
List of Tables.....	vi
Abstract.....	vii
I. Introduction.....	1
II. Theory.....	4
Luminescence.....	4
Radiative Recombination.....	4
Simple Centers.....	5
Complex Centers.....	11
Ion Implantation.....	12
Electron Beam Penetration.....	15
Past Work.....	16
III. Experimental.....	20
Sample Information.....	20
System Overview.....	21
Vacuum System.....	23
Cryogenic Transfer System.....	25
Electron Gun.....	28
Optical System.....	30
Optical Alignment.....	33
Signal Processing.....	33
Error Analysis.....	34
Etching Procedure.....	35
IV. Results and Discussion.....	37
Virgin GaAs.....	37
Unimplanted Annealed GaAs.....	37
Annealed Implanted GaAs.....	45
Effects of Electron Gun Voltage and Current on the Cathodoluminescence Spectra.....	51
Discussion.....	51
V. Conclusions and Recommendations.....	59

Conclusions.....	59
Recommendations.....	60
Bibliography.....	61
Vita.....	64

List of Figures

<u>Figure</u>	<u>Page</u>
1 Energy Band Diagram.....	6
2 Concentration of 100 keV Si in GaAs.....	13
3 System Set-up.....	22
4 Vacuum System.....	24
5 Sample Holder.....	26
6 Heli-Tran Set-up.....	27a
7 Electron Gun and Faraday Cup.....	29
8 Optical System.....	32
9 Cathodoluminescence of Virgin GaAs.....	38
10 Cathodoluminescence of Sample 4.....	40
11 Cathodoluminescence of Sample 5.....	41
12 Cathodoluminescence of Sample 10.....	43
13 Cathodoluminescence of Sample 11.....	44
14 Cathodoluminescence of Sample 6.....	46
15 Cathodoluminescence of Sample 7.....	47
16 Cathodoluminescence of Sample 12.....	49
17 Cathodoluminescence of Sample 13.....	50
18 Cathodoluminescence of Sample 5 for Varying Grid Voltages.....	52
19 Cathodoluminescence of Sample 5 for Varying Currents.....	53
20 Cathodoluminescence of Sample 5 vs. Grid Voltage	54
21 Cathodoluminescence of Sample 5 vs. Current.....	55

List of Tables

<u>Table</u>		<u>Page</u>
I	Conduction Band to Bound Transitions for Various Acceptors in GaAs.....	10
II	Spark Source Mass Spectroscopy of GaAs:Cr.....	21
III	Aging of Barium Cathode Electron Guns.....	30

Abstract

↓
Depth-resolved cathodoluminescence was performed on Si ion implanted GaAs. The samples were Cr doped semi-insulating GaAs crystals grown using the horizontal Bridgman method. Nine samples were prepared for this study, four were implanted with 100 keV Si ions at a fluence of 10^{13} cm⁻², and five were left unimplanted. One each of the implanted and unimplanted samples were annealed at 800°C for 10 minutes, 800°C for 10 seconds, 900°C for 10 minutes, or 900°C for 10 seconds, for a total of eight samples. The ninth sample was left unannealed and unimplanted as a control. Cathodoluminescence data was taken using 1000 V electrons as an excitation source. Depth resolution was achieved by taking spectral data and successively chemically etching the surface of the crystal in 250 Å steps.

No new peaks were observed in the GaAs during the experiment. Data indicated that the 900°C/10 second anneal was superior in optically activating impurities in the implanted samples. The 800°C/10 minute anneal proved to have the greatest effect in optically activating the impurities in the unimplanted samples. The 900°C/10 minute anneals exhibited spectra associated with vacancy complexes. It should be noted that the virgin GaAs control sample exhibited evidence that non-radiative processes were occurring, suppressing the spectra from the sample.

DEPTH-RESOLVED CATHODOLUMINESCENCE STUDY
OF ANNEALED SILICON IMPLANTED
GALLIUM ARSENIDE

I. Introduction

The defense electronics industry has a need for high speed specialized electronics. Often these electronics must function reliably in high temperature environments (Ref. 1). The semiconductor materials that are commonly used today cannot always meet these requirements; however, gallium arsenide (GaAs), with a higher electron mobility and a larger band gap may offer a satisfactory alternative (Ref. 14:325; 24:371).

GaAs is a crystalline material consisting of the Group III element, gallium and the Group V element arsenic. This combination yields a material with physical properties similar to Group IV elements such as silicon. GaAs has a slight ionic character giving it a higher electron mobility, and a larger band gap which increases stability by reducing the number of thermally generated free electrons in the material.

Unfortunately pure (intrinsic) GaAs must be doped with an impurity in order to be useful in semiconductor electronics. One of the most common doping techniques, diffusion, requires that the intrinsic material be raised to high temperatures (typically greater than 1000°C). The diffusion technique

is not useable on GaAs because the As in the GaAs has a high vapor pressure at high temperatures, thus As vacancies are created in the surface of the material. An alternative doping technique is ion implantation. Ion implantation has already proved useful in the production of field effect transistors, integrated circuits, microwave devices, and opto-electronic devices. The major advantages of ion implantation are:

- 1) It can be performed at room temperature.
- 2) Very high purity ions are implanted.
- 3) It allows three-dimensional control of the implant location by varying ion beam energy, size, and position (Ref. 27:627).

The major disadvantage in ion implantation is that vacancies and antisites are created by ion collisions in the crystal lattice. The damage caused by ion implantation degrades the electrical properties of the material. Damage to the crystal lattice can be partially repaired by annealing. Annealing can cause interstitial atoms to move into lattice sites thus "activating" the impurity and restoring some of the original material into the lattice sites. Annealing still may not remove all the damage and in fact the anneal may create additional damage (Ref. 24). It is necessary to understand the effects of ion implant damage and annealing on the properties of GaAs.

Cathodoluminescence is used to produce electron-hole pairs so that radiative recombination may be observed (Ref. 7).

Careful study of the spectra produced can yield information on the elements that have been "activated" and relative proportions of these elements. By etching away layers of the material the effects of implant and anneal damage, and concentration of the impurities may be observed as a function of depth in the crystal.

The objective of this study was to investigate the effects of annealing on Si ion implanted GaAs as a function of depth. Cathodoluminescence was the excitation method. The crystals studied were grown using the horizontal Bridgman method. Four samples were implanted with 100 keV Si at a fluence of 10^{13} cm^{-2} . Five samples were left unimplanted. One implanted and one unimplanted crystal each were annealed at 800°C for 10 minutes, 800°C for 10 seconds, 900°C for 10 minutes, and 900°C for 10 seconds. The fifth unimplanted sample was left undoped and unannealed as a control. For each sample cathodoluminescence spectra were recorded from 8000 \AA to 9777 \AA . The samples were then chemically etched and another spectrum taken. This process was repeated until about 750 \AA of material had been removed. Locations of peaks in the spectra were found, and normalized magnitudes of the peaks were plotted as a function of etch depth.

II. Theory

To interpret the data taken during this study it is necessary to have an understanding of the basic theories on luminescence, radiative recombination, ion implantation, and electron beam penetration. The following information provides a background for this thesis, and assumes a basic understanding of band theory. Readers are referred to the various texts on these subjects for additional information.

Luminescence

Luminescence can be produced by bombarding the crystal lattice with electrons or photons producing electron-hole pairs. The intensity of the excitation source is attenuated as it penetrates into the crystal. Because of this attenuation most of the energy is absorbed near the surface of the crystal. Electron-hole pairs will tend to diffuse away from the excited area in order to restore medium homogeneity. Self-absorption of emitted radiation in this region and the lower probability of self-absorption in those regions already excited indicates that radiation from recombination will most likely leave through the excited surface (Ref. 4:182).

Radiative Recombination

Electron-hole pairs can exist in different states depending on the state of the electron and hole. Decay of the

electron-hole pair from a higher state to lower energy state will be accompanied by the emission of a photon with the energy difference between the two states. Luminescence spectra from the crystals can contain many lines because of the many possible energy states in the crystal. Radiative recombination in GaAs can be broken into two categories: simple centers and complex centers,

Simple Centers. A simple center can be thought of as an impurity in a lattice site which can be modeled using hydrogen type energy states. Figure 1 represents the possible recombination schemes for simple centers. These recombinations include: free electron-free hole recombination, exciton annihilation, free electron-bound hole recombination, and bound electron-free hole recombination.

Line A in Fig. 1 represents the free electron-free hole recombination. The energy of this transition is given by:

$$E(h\nu) = E(\text{Gap}) + 2kT \quad (1)$$

where

$E(h\nu)$ = the energy of the photon

$E(\text{Gap})$ = the energy of the gap between the conduction band and the valence band (1.521 eV at 21°K)

k = Boltzmann's constant, 8.61708×10^{-5} eV/°K

T = temperature in degrees Kelvin

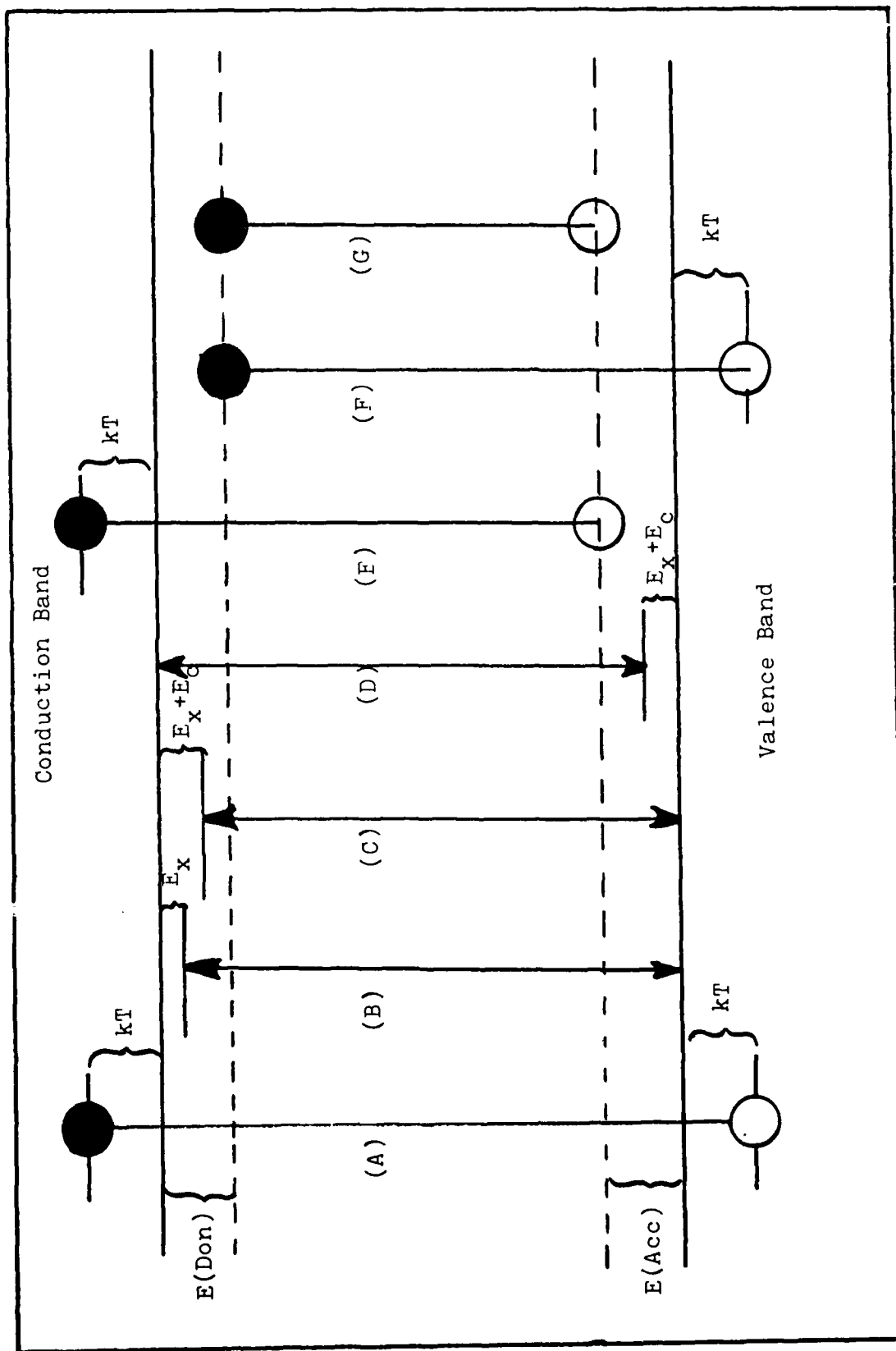


Fig. 1. Simple Energy Band Diagram

The effect of the $2kT$ term is to increase the photon energy with increasing temperature, and is a consequence of the kinetic energy of the free electron and the free hole (Ref. 3:1042; 7:7). In actuality the temperature term is rather small compared to $E(\text{Gap})$ and is only 0.819 meV at 9.5°K . The free electron-free hole recombination has not yet been observed in bulk grown GaAs and all estimates of band gap energy are made from observed exciton transitions (Ref. 36:386).

Line B of Fig. 1 represents the annihilation of a free exciton. An exciton may be thought of as an electron and a hole which are bound together through coulombic attraction. A free exciton is one which is not bound to a lattice site and therefore free to move through the lattice. The exciton has a slightly lower energy than the free electron-free hole due to forces binding the electron and hole into an exciton (Ref. 21:504). At 2°K this recombination appears at 1.5156 eV in GaAs (Ref. 36:342) slightly less than the band gap energy. The full width at half maximum of the free-exciton recombination is approximately 1meV, and the energy and shape of the emission line is independent of impurity concentration (Ref. 36:387). A formula for calculating the energy released during free exciton recombination including the temperature dependence is given by Pierce (Ref. 30:38).

Line C of Fig. 1 represents the recombination of an exciton bound to a donor site. Line D represents the

recombination of an exciton bound to an acceptor site. Because the exciton is now bound to a lattice site, in both cases, the energy emitted from the recombination is lower than that of the free exciton (Ref. 4:299). Since the exciton is now bound to a lattice site it has no motion with respect to the rest of the lattice and therefore no direct temperature dependence exists for the recombination energy (Ref. 30:39). Silicon doped GaAs at 2°K exhibits three bound exciton lines:

- 1) exciton bound to a neutral donor.....1.5145 eV
- 2) exciton bound to an ionized donor.....1.5135 eV
- 3) exciton bound to an acceptor.....1.5125 eV

Bound exciton emissions in general have slightly narrower emission lines than free excitons.

Line E of Fig. 1 represents a free electron-bound hole recombination. The energy of this recombination is given by

$$E(h\nu) = E(\text{Gap}) - E(\text{Acc}) + kT + nE(\text{ph}) \quad (2)$$

where

$E(\text{Acc})$ = acceptor energy level (30 meV for Si in GaAs at 20°K)

n = number of phonons which assist the transition

$E(\text{ph})$ = phonon energy, 36 meV for the longitudinal optical phonon in GaAs (Ref. 36:388)

The last term in Eq. 2, $nE(\text{ph})$, represents the discrete amount of energy that can be absorbed or given up through

lattice vibrations. The free electron-bound hole recombination also exhibits a thermal dependence but the temperature term is only half that of the free electron-free hole temperature term since only the electron is free to move in the lattice. Energy level differences for different acceptors are generally large enough to identify the acceptors in GaAs. Table I lists energies for the free electron-bound hole recombination for a variety of acceptors at 5°K (Ref. 3:1051; 32:1111).

Line F of Fig. 1 represents the bound electron-free hole recombination with the electron bound to a donor. The energy level of donors in GaAs are so close together that it is not possible to distinguish one donor from another. The equation for the bound electron-free hole recombination energy is the same as that of the free electron-bound hole recombination except that $E(\text{Acc})$ is replaced by $E(\text{Don})$, The donor energy level. For Si doped GaAs, $E(\text{Don})$ is 6.8 meV and a peak at 1.5137 eV is attributed to this type of transition (Ref. 36:342).

Line G of Fig. 1 represents a bound electron-bound hole recombination. The recombination energy is given by (Ref. 36:335; 9:744):

$$E(h\nu) = E(\text{Gap}) (E(\text{Acc}) + E(\text{Don})) + \frac{e^2}{\epsilon R} \quad (3)$$

where

e = the charge of an electron

TABLE I

CONDUCTION BAND TO BOUND
TRANSITIONS FOR VARIOUS
ACCEPTORS IN GaAs

Acceptor	Transition Energy
Carbon	1.4935, 1.4939
Silicon	1.4850, 1.4902
Germanium	1.4790
Tin	1.3490
Zinc	1.4888
Cadmium	1.4848
Beryllium	1.4915
Magnesium	1.4911

ϵ = the dielectric constant of the crystal (GaAs)

R = the spacing between interacting donor-acceptor pairs

Since the electron and hole are bound to impurities which must occupy lattice sites, R takes on discrete values based on the crystal lattice. The recombination energy will also take on discrete values. The recombination should yield a series of discrete luminescence lines with lines arising from larger R values being less intense since those recombinations are less probable (Ref. 36:335). In fact only one peak has been seen around 1.485 eV at 20°K (Ref. 6:1000). This transition occurs at a point where R is so large that the individual lines

overlap and Eq. 3 becomes:

$$E(h\nu) = E(\text{Gap}) - (E(\text{Acc}) + E(\text{Don})) \quad (4)$$

Complex Centers. Complex centers are associated with emission lines of lower energy than simple centers that cannot be explained using the simple model of hydrogen type energy states used for simple centers. A complex center is formed from impurities and/or lattice vacancies. Because its energy is so much deeper into the forbidden region of the band gap, complex centers are often referred to as deep centers. A complex center might be an impurity close enough to a vacancy or other impurity to form a complex having its own properties and energy states (Ref. 35:1663). Since complex centers do not conform to any periodicity in the lattice and have various energies, they cannot be modeled using simple hydrogen type energy states. Complex centers are most commonly associated with lattice vacancies or transition metals and precipitates in the crystal (Ref. 36:359). The literature is in constant disagreement as to the nature of complex centers in GaAs, but the following peaks at 1.41 and 1.36 eV are generally associated with vacancy complexes in GaAs:Si (Ref. 5:622). Another peak at 1.44 eV is believed to be associated with a gallium antisite (a gallium on an arsenic site) (Ref. 34:155). An emission associated with a complex center and referred to as the Q band by Swaminathan was found to have an energy which fluctuated between 1.39 and 1.47 eV depending on Si concen-

trations, annealing temperatures, and capping conditions (Ref. 31).

Ion Implantation

Ion implantation has become a common method of doping GaAs for several reasons (Ref. 25:627):

- 1) It can be performed at room temperature.
- 2) A high purity of dopants can be obtained.
- 3) A three-dimensional doping profile can be obtained by controlling beam size, position, and energy.
- 4) Almost any element can be used as a dopant.

Ion implantation involves choosing a dopant, purifying it, ionizing it, and accelerating it towards the target material. The ions will collide with other atoms in the lattice, losing energy until they come to rest. The energy lost to the lattice is dependent on many factors such as the ion type, the lattice density, the lattice atom, the initial ion energy, and the collision cross-sections. The process by which an ion comes to rest in the lattice is purely random. Because of this randomness the final distribution of the dopant can be expressed as a depth profile. The implant profile of 100 keV Si ions in GaAs (Figure 2) was predicted using the range distribution theory developed by Lindhard, Scharff, and Schiott (LSS) (Ref. 23). Fig. 2 has a Gaussian peak at 850 Å with a standard deviation of 442 Å. More information on the LSS theory can be found in the lengthy work by Gibbons (Ref.15).

Unfortunately the collisions of ions with atoms in the

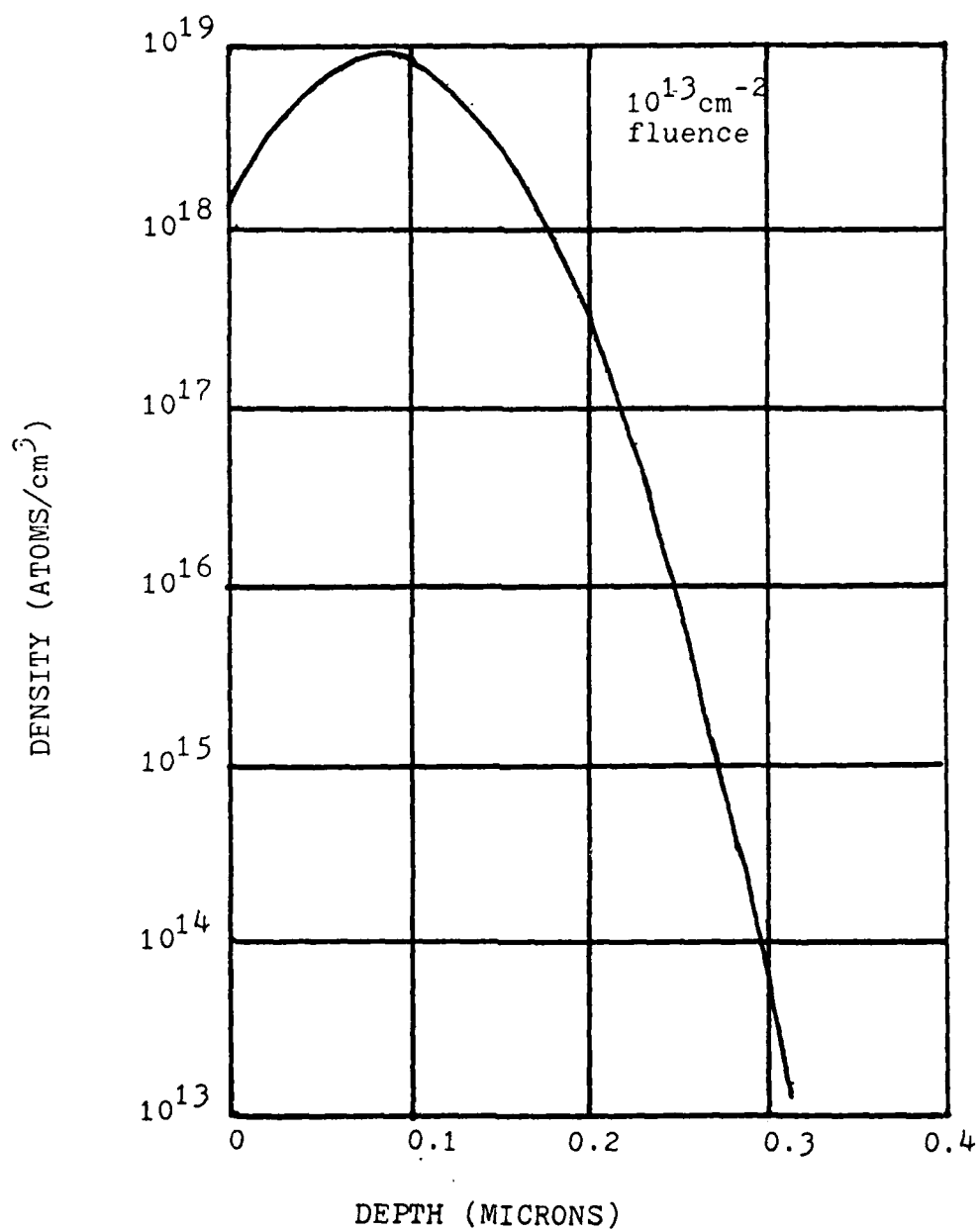


Fig. 2. Concentration of 100 keV Si in GaAs

lattice creates vacancies and other lattice defects.

The displaced atoms become part of the damage mechanism, knocking other atoms out of their sites. Thus an area of damage is created around the ion's path in the crystal. The type of damage created depends on several factors including the ion's mass and energy (Ref. 27:627). Studies using GaAs and other dopants found that the lattice defects extended approximately 1 μ m farther into the material than predicted (Ref. 15:848; 28:5765; 2:405). Key found that damage from 120 keV Si affected the 1.49 eV peak as far as 3200-4000 Å into samples similar to ones used in this study.

Implant damage in GaAs can reduce luminescent intensity for some types of transitions (Ref. 15:25;26) and it is believed that additional non-radiative mechanisms are introduced into the material. Annealing has proven effective in increasing luminescent intensity due to activation of the implant (Ref. 22); however, annealing has some major disadvantages (Ref. 8:568). Some of those disadvantages are:

- 1) Depletion of arsenic from the surface at temperatures above 650°C if the surface is not properly capped.
- 2) Diffusion of defects and implant ions further into the crystal than the original implant region.

Because annealing can affect the activation of the implant and repair vacancy damage in the crystal, it is necessary to study the effects on unimplanted and implanted crystals under different annealing conditions and compare the results to those

of Maclin and DeForest (Ref. 12;24).

Electron Beam Penetration

Electron penetration in the crystal lattice is similar to ion penetration except that interactions occur mostly with other electrons in the lattice. The penetration profile of electrons is Gaussian just as it was for ions. Modeling of penetration is simpler if only electron-electron interactions are considered.

Studies at electron beam energies of 1 keV, as were used in this study, are not common. Most studies tend to use higher energy electrons. Feldman worked with electron beam energies in the 1 keV range (Ref. 14). Using data obtained from normal incidence penetration of electrons with various materials, he empirically derived the equation:

$$R = bE^r \quad (5)$$

where

R = the penetration depth of the electrons (the peak of the Gaussian)

E = the energy of the electrons in keV

b and r are constants of the material

Martinelli and Wang studied GaAs with electrons in the range of 3 to 7 keV (Ref. 25). They fit their results to Eq. 5 and found b and r were 270 Å and 1.46 respectively.

Penetration depths at 45° have been shown to be within 10% of penetration depths at normal incidence (Ref. 28:3209). For this study it is assumed that penetration at 45° is approximately the same as at normal incidence. Thus for 1 keV electrons the penetration depth is 270 Å and for 1.2 keV electrons the penetration depth is 352 Å.

Past Work

It is appropriate at this point to discuss some of the work already done on GaAs.

Chatterjee studied the native defects of heat treated (850°C) Cr doped GaAs under various environmental conditions (Ref. 9). Four spectral lines were found, a band to band recombination at 1.518 eV and three peaks at 1.47, 1.35, and 1.33 eV associated with defects in the material caused by the annealing. The peak at 1.47 eV was determined to be an arsenic vacancy complex since arsenic has a high vapor pressure, and this peak showed a large increase in intensity when the crystal was annealed under vacuum, and was suppressed when annealed with a SiO_2 cap. The peaks at 1.35 and 1.33 eV were associated with Ga vacancy complexes since these peaks were greatest with the SiO_2 cap, and SiO_2 has been shown to attach Ga.

Birey and Sites studied the spectra of Si doped GaAs annealed between 550 and 700°C for periods of 10 to 150 minutes in an H_2 atmosphere. They identified five transitions using photoluminescence for samples at 12°K . The first

transition was at 1.514 eV and was associated with a donor-valence band transition. The second transition was at 1.486 eV and was associated with a donor-acceptor transition. The third transition occurred at 1.2 eV in heavily doped samples and was believed to be associated with a $\text{Si}_{\text{Ga}}\text{-V}_{\text{Ga}}$ complex. The fourth transition occurred at 1.36 and 1.33 eV. The 1.36 eV transition was believed to be associated with a $\text{V}_{\text{As}}\text{-Si}_{\text{As}}$ complex and the 1.33 eV transition was its phonon replica. The fifth transition occurred at 1.44 eV and was associated with a $\text{Si}_{\text{Ga}}\text{-Si}_{\text{As}}$ complex.

Swaminathan studied n^+ Si doped and semi-insulating Cr doped GaAs after heat treating at 780 to 830°C in H_2 for 2 to 15 hours. Spectra were taken with the samples at 5.5°K. A band was identified at 1.492 eV associated with a free to bound transition. A band which Swaminathan called the Q band was observed at 1.44 eV, and a band at 1.41 eV was also observed which he called the R band. Both the R and the Q band were associated with vacancy complexes and showed strong dependences on sample temperature and excitation intensity (Ref. 34).

Maclin studied the effects of annealing Si ion implanted GaAs using depth-resolved cathodoluminescence and photoluminescence. Luminescence at various depths in the material was observed by etching off the surface of the crystal with an ion beam. He found that ion etching created additional lattice damage which affected the luminescence measurement. The Si ion was implanted with a 10^{14} cm^{-2}

fluence at 120 keV which gives a peak penetration depth of 1025 Å with a 510 Å standard deviation. It was found that a dead layer existed in unannealed samples to about 760 Å into the crystal. For the sample annealed at 900°C for 15 minutes a large peak appeared at 1.441 eV at the surface which quickly disappeared as he etched into the crystal and was replaced by a peak at 1.494 eV after the 1015 Å etch (Ref. 24).

DeForest studied unannealed Si ion implanted GaAs using depth-resolved cathodoluminescence and photoluminescence also. However, he used a chemical etch technique rather than ion etching to avoid creating further lattice damage. He found that the ion implantation without being annealed reduced the intensity of the 1.49 eV transition. In fact a "dead" layer in which little or no luminescence was observed. This dead layer extended 1100 Å into the crystal for implant fluences of 10^{12} cm⁻² and 3700 Å for fluences of 10^{15} cm⁻².

Pomrenke at the Avionics Laboratory (AFWAL) examined the Q band discussed by Swaminathan. He found that fluctuations in the Q band energy were caused by varying the doping procedure, dosages, anneal temperature, and capping conditions. He concluded from his data that this band was probably the result of three different processes which competed against each other in the substrate. The processes at $V_{As}-Si_{As}$, Ga_i-Si_{As} , and $Si_{Ga}-Ga_{As}$. He assumes that at lower energies near the surface of the crystal the $V_{As}-Si_{As}$ recombination is dominant while deeper into the crystal the shift to

higher energies is a result of the $\text{Ga}_i\text{-Si}_{\text{As}}$ recombination being dominant.

III. Experimental

This section deals with the equipment and procedures used to obtain the results discussed in the next section. The order of presentation is: Sample Information, System Overview, Vacuum System, Cryogenic Transfer System, Electron Gun, Optical System, Optical Alignment, Signal Processing, and Etching Procedure.

Sample Information

The GaAs samples used in this study were all high-purity semi-insulating chromium compensated bulk material grown by the horizontal Bridgman method. Samples were purchased from Crystal Specialties Inc., batch #CS E-119. Each sample measured $\frac{1}{4}$ inch by $\frac{1}{4}$ inch. Samples were all etched with a 1:1:3 solution of 30% H_2O_2 : H_2O : H_2SO_4 for one minute to remove the surface damage caused by chemo-mechanical polishing performed by the manufacturer. This etch removed approximately 1.25 μm of the material.

Four samples were then implanted with 100 keV silicon ions at a fluence of 10^{13} cm^{-2} . One implanted and one unimplanted sample each was then taken, capped with a 1000 Å SiN_4 coating, and annealed for 800°C and 10 minutes, 800°C and 10 seconds, 900°C and 10 minutes, and 900°C and 10 seconds, for a total of eight samples. A ninth sample of virgin GaAs:Cr was left undoped and unannealed as a control. A spark source mass spectrographic analysis of the virgin

TABLE II

SPARK SOURCE MASS
SPECTROSCOPY OF GaAs:Cr
CS E-119

<u>ELEMENT</u>	<u>ppmA</u>
Iron	0.5
Magnesium	0.01
Chromium	0.1
Silicon	0.3
Aluminum	0.03
Boron	0.01

GaAs:Cr was performed by Wright State University, Dayton, Ohio, for AFWAL/AADR. The major impurities found are summarized in Table II. The 10 minute annealed samples were annealed in an H_2 atmosphere in a standard annealing furnace. The 10 second annealed samples were annealed in an N_2 atmosphere in a pyrolytic oven. The rise time of the pyrolytic oven was 9 seconds and then the samples were left in another 10 seconds before turning off the heater. Samples were placed with the implanted surface down on the graphite heating element.

System Overview

Figure 4 represents the basic set up for data taken in

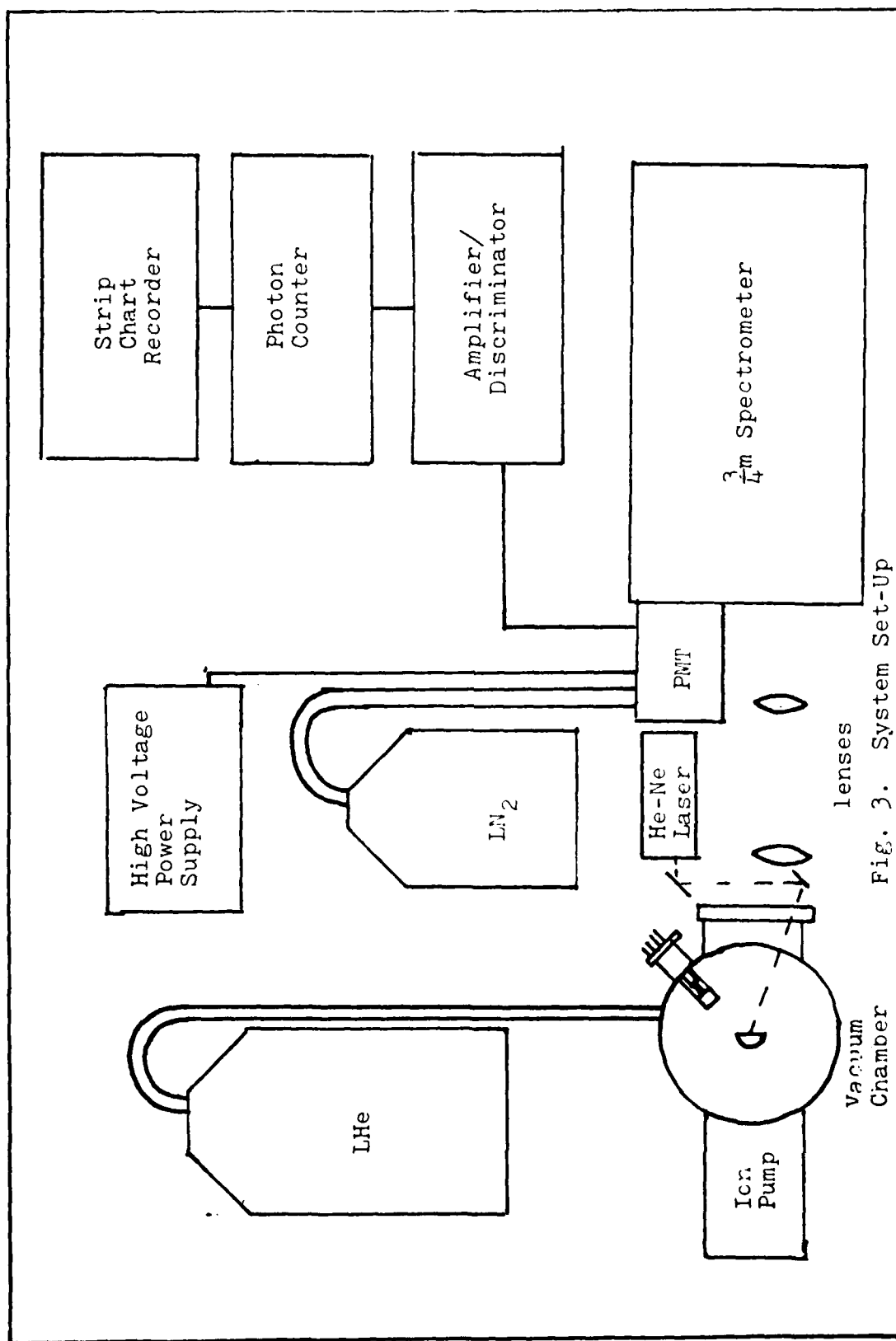
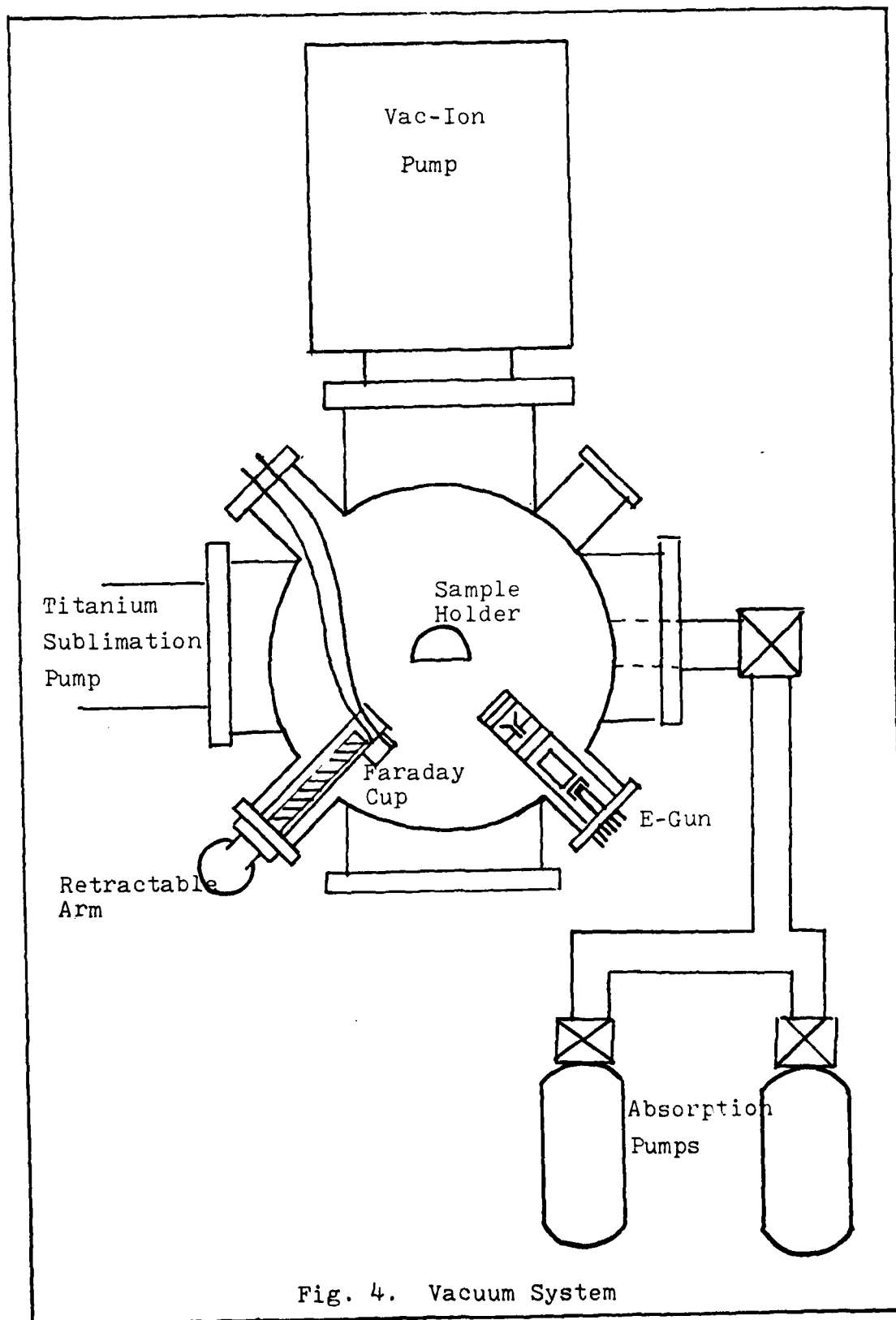


Fig. 3. System Set-Up

this study. The samples were mounted on the heli-tran cold finger placed in the vacuum system and pumped down to 8×10^{-8} torr using a vac-ion pump and absorption pumps. An electron gun was used as the excitation source for the cathodoluminescence data taken in this study. A HeNe laser was used for alignment of the components in the optical system. The luminescence from the sample was collected by the two lenses in the system and focused on the slit of the spectrometer. A cooled photomultiplier which converted luminescence to an electrical signal was mounted at the exit slit of the spectrometer. This signal was then processed by an amplifier-discriminator and photon counter and recorded with a strip chart recorder to obtain a hard copy of the data.

Vacuum System

The vacuum system used in this study is represented in Figure 5. The vacuum chamber measured 12 inches in diameter and stood approximately 2 feet tall. The top half of the chamber had four eight inch ports spaced 90° apart, and four $2\frac{3}{4}$ inch ports also space 90° apart and offset 45° from the eight inch ports. In the top of the chamber was a $2\frac{3}{4}$ inch port in which the heli-tran was mounted. Two of the eight inch ports were blanked off. Mounted to one eight inch port was an electron gun not used in this study. Mounted to the other eight inch port was a quartz window. The electron gun used in this study was mounted in one of the $2\frac{3}{4}$ inch ports



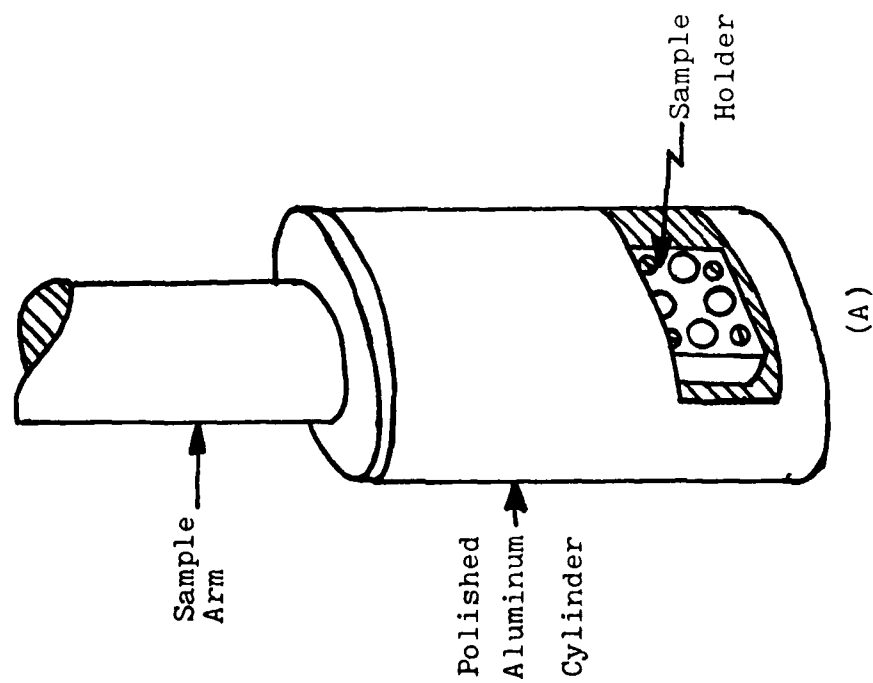
next to the quartz window. The Faraday cup translation mount was in another $2\frac{3}{4}$ inch port and the electrical feedthroughs for the Faraday cup were mounted in another $2\frac{3}{4}$ inch port. The last $2\frac{3}{4}$ inch port was unused.

The vacuum system was roughed down to below 1 m using two Varian absorption pumps at which time the high vacuum valve between the absorption pumps and the chamber were closed. A 110 liter per second Varian model 92/0041 vac-ion pump was then started which would pump the system down into the mid 10^{-8} torr range. If necessary a titanium sublimation pump was used to assist in pumping.

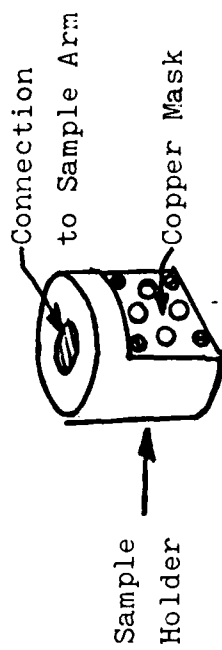
Cryogenic Transfer System

The cryogenic transfer system can be broken down into two parts, the heli-tran and the sample holder.

The sample holder, Figure 5, was mounted in the same horizontal plane as the electron gun and the quartz window. The sample holder was machined from a solid block of copper in the shape of a half cylinder. The samples were mounted on the flat face of the sample holder and held in place by a copper mask with four 5 mm diameter holes so that all but the corners of the sample were covered. The sample mount also held a GaAs diode, a gold-chromel thermocouple, and a resistance heater. The GaAs diode, the resistance heater, and a Lakeshore Crotronics model DTC 500 cryogenic temperature controller provided precision control of the temperature of the sample holder. The gold-chromel thermocouple was connected to an Instrulab 5000 temperature indicator which



(A)



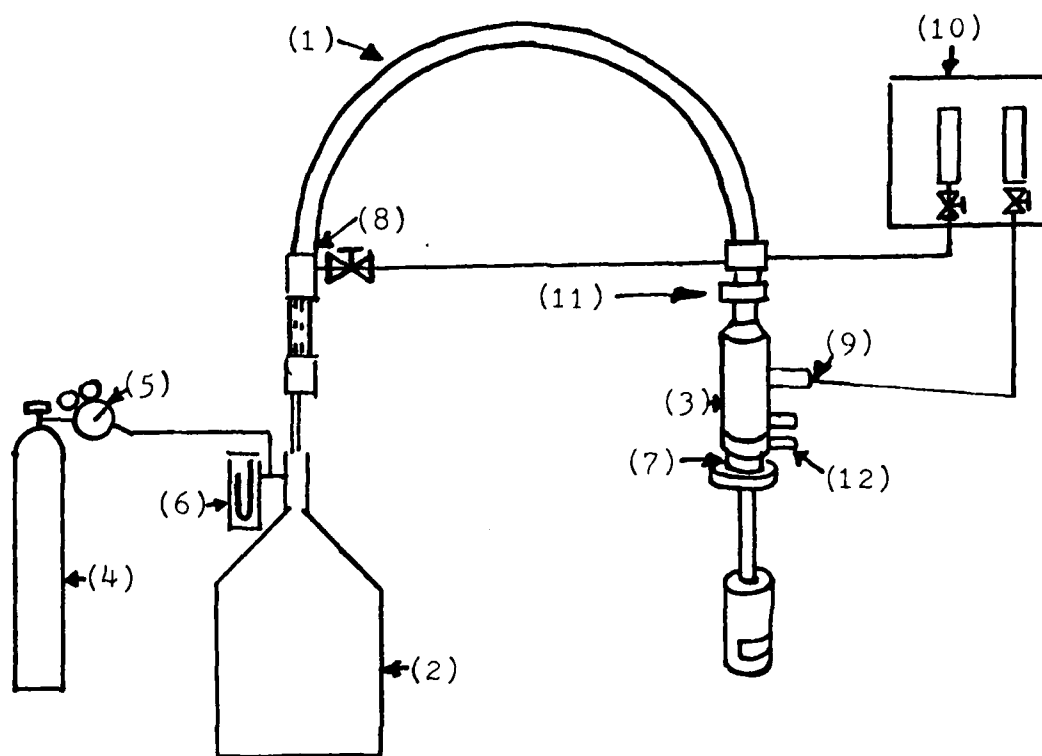
(B)

Fig. 5. (A) Sample Arm and (B) Sample Holder

provided a digital readout of the sample holder's temperature. Over the sample holder was mounted a polished aluminum cylinder with a rectangular window cut out over the samples. The cylinder provided shielding of the samples from extraneous radiation sources.

The liquid helium transfer line, an Air Products and Chemicals model LT3-110 Liquid Transfer Heli-Tran, Figure 6, provided cooling for the sample holder. The heli-tran consisted of a transfer tube, the tip flow surrounded by two interconnected transfer jackets, and the shield flow, all enclosed in vacuum. The liquid helium dewar was pressurized to force the liquid helium into the tip and the shield flow. The tip flow travels to the sample holder and exits just above the sample arm. The shield flow travels in the inner jacket to the sample holder and then returns in the outer jacket to the dewar where it is exhausted. The exhausted helium from the tip and the shield flows are transferred to two flow control valves. Tip flow and shield flow may be controlled to some extent using the two flow control valves. Tip flow may also be adjusted using the needle valve on the sample arm. Typical temperatures obtained for the sample holder were 8.5° to 9.5°K .

The cooldown procedure was as follows. The liquid helium dewar was pressurized to 4 PSI using a K-bottle of oil free helium. The tip of the transfer line was inserted just inside the dewar and the tip and shield flow control valves were wide open. This procedure purged the transfer line of air



1. Helium Transfer Hose
2. Liquid Helium Dewar
3. Heli-Tran Cold End (Sample Arm)
4. Gaseous Helium Cylinder
5. Pressure Regulator
6. Pressure Gauge on Helium Dewar
7. Sample Cell Inlet Tube
8. Shield Flow Vent
9. Tip Flow Vent
10. Accessory Flow Control Panel
11. Micrometer Valve Adjustment
12. Transfer Hose Evacuation Port

Fig. 8. Heli-Tran Setup

and water vapor so it wouldn't freeze up. After 5 minutes the transfer line was lowered the rest of the way into the dewar and helium transfer was begun. As the transfer line was lowered into the dewar continuous venting was necessary to keep the dewar pressure below 5 PSI as the warm transfer line contacts the liquid helium. Typically the system took 45 minutes to cooldown to 9.5°K. At 200°K the heater jacket was plugged in to prevent exhaust line freeze up.

When a run was finished it was necessary to allow the sample holder to warm up to room temperature before removing it from the vacuum system to prevent the sample holder from icing over. Typically this took about 3 hours.

Electron Gun

A standard RCA electron gun with a barium oxide cathode was used for the cathodoluminescence electron source. Figure 7 is a diagram of the gun. After installing the gun with a new filament and cathode it was necessary to "age" the gun in order to activate the barium oxide cathode. Table III is the aging schedule for the electron gun. Whenever the vacuum system was opened it was necessary to apply several amps to the filament and maintain the vacuum chamber at a positive pressure with respect to atmosphere using dry N₂ to prevent air from degrading the gun.

During operation the grid, cathode, and filament were floated at a -1000 V potential using a Keithley model 240 power supply. The focus electrode was floated at a -800 V

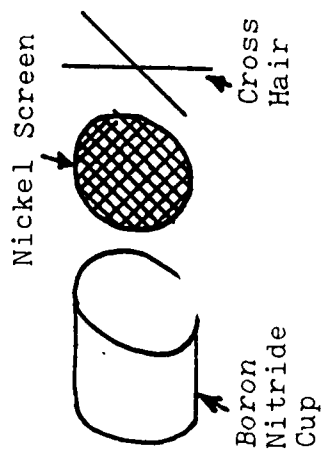
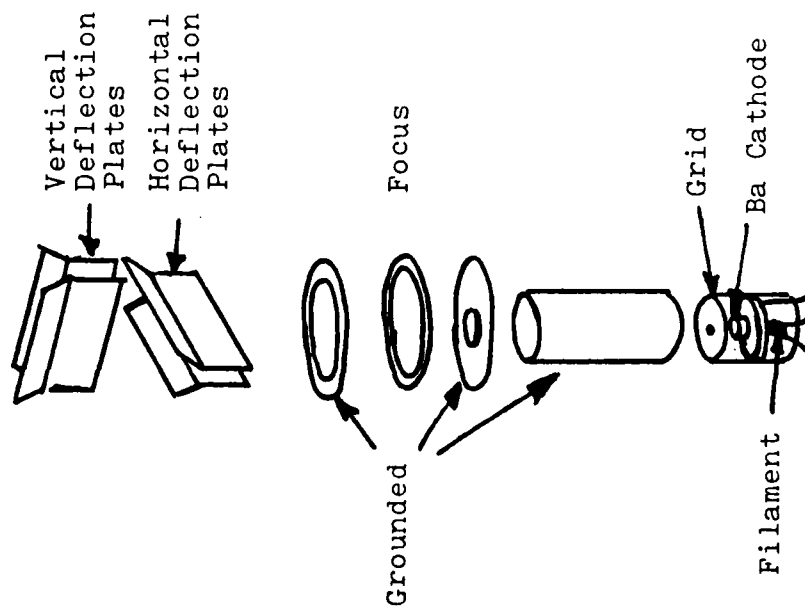


Fig. 6. Major Components of (A) Electron Gun and (B) Faraday Cup

TABLE III
AGING OF BARIUM CATHODE ELECTRON GUNS

Time	Filament Voltage	Grid Voltage	Focus Voltage
1 min.	6.3	0	0
1.5 min.	12.5	0	0
10 min.	9.0	+5 0	150
15 min.	9.0	0	0
5 min.	6.3	0	0

potential. Other components in the gun were kept at ground potential. The voltage for the deflection plates was provided by three 45 volt dry cell batteries with a center tap to system ground. Most cathodoluminescence data was taken with the grid at -1000 V and 72 amps into the Faraday cup. The Faraday cup was mounted on a retractable arm and had a screen over the entrance of the cup kept at -90 V with respect to the rest of the cup in order to suppress secondary electrons. Output of the Faraday cup was measured using a Keithley model 410 Micro-Microammeter.

Optical System

The optical system consisted of two quartz lenses. The first lens was 4.5 cm in diameter and had a focal length of 25 cm; the second lens was 3.5 cm in diameter and had a focal length of 15 cm. The first lens was located approximately one focal length from the sample, and provided a fairly

collimated output of the sample luminescence. The second lens focused the collimated light onto the slit of the spectrometer, Figure 8. The focal lengths of the lenses were chosen such that the luminescence would slightly overfill the spectrometer grating. The actual distances varied slightly depending on which sample was being looked at.

A Spex Industries Model 1702 three-quarter meter Czerney-Turner spectrometer with a 1200 line/mm grating blazed at 5000 \AA was used in the study. The Spex 1702 had entrance and exit slits which were adjustable from 5 mm to 4 mm. Most of the spectra were recorded using a $500 \mu\text{m}$ slit; however, some samples exhibited a stronger luminescence than others and for those $100 \mu\text{m}$ slits were used. Slit size was the limiting factor in the spectrometers resolution. Using the numbers given in the Spex manual at 8273 \AA (1.499 eV) the calculated resolution was $\pm 2.55 \text{ \AA}$ (0.0005 eV) with $500 \mu\text{m}$ slits or $\pm 0.51 \text{ \AA}$ (0.0001 eV) with $100 \mu\text{m}$ slits.

The light passing through the exit slit was collected by an EMI 9808B photomultiplier tube (PMT) with an S-1 photocathode and 14 beryllium-copper, linear focusing dynodes. The PMT operated in the 3000 \AA to 11000 \AA range. The PMT was housed in a Products for Research TE 114 photomultiplier housing which could be cooled with liquid nitrogen (LN_2). The PMT was kept at -50°C by flowing LN_2 through the PMT housing and regulating the flow with a Products for Research LN_2 Cryostat Controller. The voltage applied to the PMT was -2000 V using a Keithley model 244 High Voltage

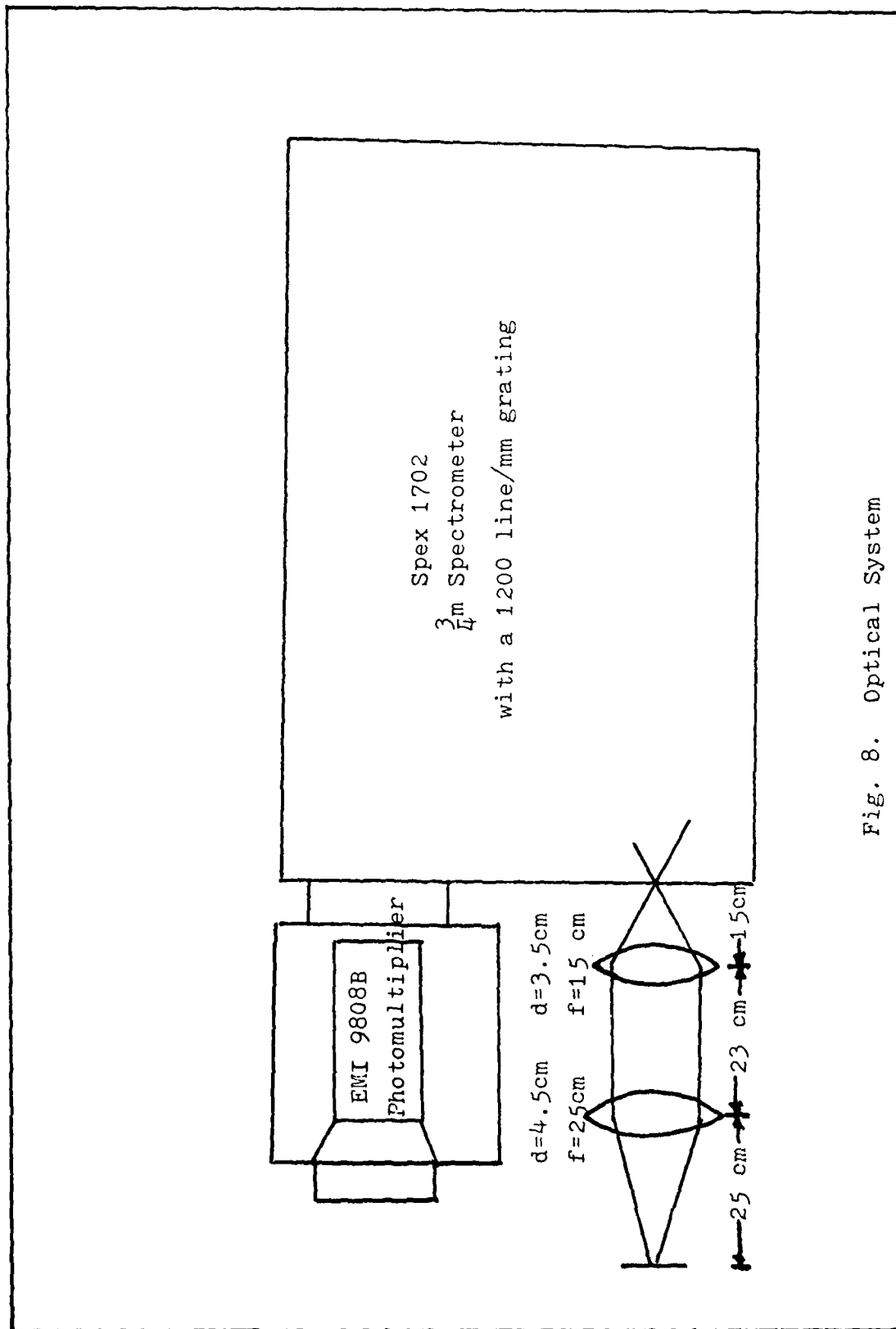


Fig. 8. Optical System

Power Supply. It was determined that -2000 V on the PMT produced the best signal to noise ratio with this tube. Typical dark counts measured with this system were approximately 102 counts per second.

Optical Alignment

The method used for aligning the optics was relatively simple. The voltage was adjusted on the vertical and horizontal deflection plates on the electron gun until the cathodoluminescence spot was centered on the sample. The 2.5 mW HeNe alignment laser output was then overlayed onto the cathodoluminescence spot. The scattered HeNe light was collected by the 25 cm lens and the position of the lens was adjusted until the output was collimated. The 15 cm lens was then placed in the optical train, and its position was adjusted until there was a focused spot of HeNe light on the spectrometer entrance slit. With the spectrometer set to 8325 Å (1.49 eV) the position of the 15 cm lens was adjusted to maximize the signal from the PMT.

Signal Processing

The signal from the PMT was sent through a Princeton Applied Research Model 112 Amplifier/Discriminator. The amplifier/discriminator amplifies the signal from the PMT and in addition an adjustable "window" allows the user to reject the noise signal originating in the PMT and amplifier by eliminating signal with the wrong temporal properties.

The output of the amplifier/discriminator is a series of 5 nanosecond pulses whose frequency depends in the input signal level. The pulses are passed to a Princeton Applied Research Model 1112 Photon Counter/Processor. The photon counter counts the pulses and displays the digital data at a rate between 1 second and 999 seconds. The photon counter is capable of recording a background count rate (dark counts) and subtracting it from the signal. A digital to analog converter allows the output of the photon counter to be recorded on a strip chart recorder (a Houston Instruments Omnigraphic 2000 Recorder in this case) for a hard copy of the data. The photon counter was set to count for 0.5 second periods with the accumulated counts at the end of that 0.5 second period being recorded on the strip chart recorder. The strip chart recorder advanced at a rate of 142.5 seconds per inch \pm 1.304 seconds per inch. This yields a resolution of \pm 0.5 Å (0.00009 eV) at a spectrometer scan rate of 50 Å per minute. Given these operating parameters the chart output was 46.75 Å per cm.

Error Analysis

It is convenient at this point to determine the uncertainty in the data which has been taken using the apparatus described in the previous sections.

The energy of a given peak on the strip chart is given by:

$$E(\text{eV}) = 12395 / (L \times \text{SCS} \times \text{SS} + 8006.2) \quad (6)$$

where

$E(\text{ev})$ = peak energy in eV

L = the distance in cm between the 8006.2 reference line and the peak ($3.95 \text{ cm} \pm 0.025 \text{ cm}$ for the 1.515 eV peak)

SCS = the strip chart speed ($0.935 \text{ minutes/cm} \pm 0.007$)

SS = the spectrometer scan speed ($50 \text{ \AA/min.} \pm 0.01$)

The deviation computed using these numbers yields an error of $\pm 0.0096 \text{ eV}$ in the values computed for peak energies.

Etching Procedure

In order to perform depth resolved studies of GaAs it is necessary to etch off the surface material after a spectrum has been taken. There are two types of etching that could be performed, ion etching and chemical etching. Ion etching has been shown to cause additional damage to the crystal thus interfering with the quality of the cathodoluminescence spectra (Ref. 24). For this study chemical etching was used.

DeForest used a 1 ml:1 ml:500ml, 30% $\text{H}_2\text{O}_2:\text{H}_2\text{SO}_4:\text{H}_2\text{O}$ etch solution at 3°C and 23°C (Ref. 35). This solution was shown to etch at a rate of 300 \AA/min. at 3°C . This was deemed unsatisfactory in this study since small errors in etching time produced large errors in the etch depth. The etching solution used in this study was a 1 ml:1 ml:250 ml solution of 30% $\text{H}_2\text{O}_2:\text{H}_2\text{SO}_4:\text{H}_2\text{O}$ used by Gernot Pomrenke at AFWAL/AADR (Ref. 31). This solution etched GaAs at a rate of 36.1 \AA/min.

at 1.3°C. The H_2O_2 was kept refrigerated and in the dark to prevent degradation during the study. Once the solution was mixed it was placed in an ice bath and chilled to 1.3°C. Samples were then immersed in the solution for a period of 6 minutes and 55 seconds which removed 250 Å of the material. The samples were then immersed in 18 megohm water to halt the etching process. Samples were cleaned, dried, and placed in their containers. Two pieces of crystal were used for each sample, one piece was used to acquire the spectra, the other piece was partially covered with black wax and was used as an etch reference. Both pieces were always etched simultaneously. When this study was completed the wax was removed from the reference pieces, and the total etch depth of each sample was measured using a Sloan Dektak Surface Profile Machine.

IV Results and Discussion

The data obtained in this study can be broken down into four distinct sections which I will discuss separately. These sections are: Virgin GaAs, Unimplanted GaAs, Implanted Annealed GaAs, and The Effects of Electron Gun Voltage and Current on the Cathodoluminescence Spectra.

Virgin GaAs

The virgin GaAs, Figure 9, exhibited a weak spectrum compared to other samples in this study. Two lines were visible at $1.514 \text{ eV} \pm 0.009$ and $1.489 \text{ eV} \pm 0.009$. The peak at 1.514 eV has the same energy as that of a bound exciton annihilation. The peak at 1.489 eV corresponds to a conduction band to bound acceptor transition. It is assumed that the acceptor is Si since the major impurities in the virgin material were Fe, Cr, and Si. Fe and Cr are deep level acceptors leaving only Si with an energy in this region. The 1.489 and the 1.514 eV lines are the only lines that appeared in the spectrum. Three separate spectra were run, one at the surface of the crystal, one after a $1.25 \mu\text{m}$ etch, and one after etching in a total of $2.57 \mu\text{m}$. None of these spectra exhibited any significant difference from one another.

Unimplanted Annealed GaAs

(There were four samples of unimplanted annealed GaAs used

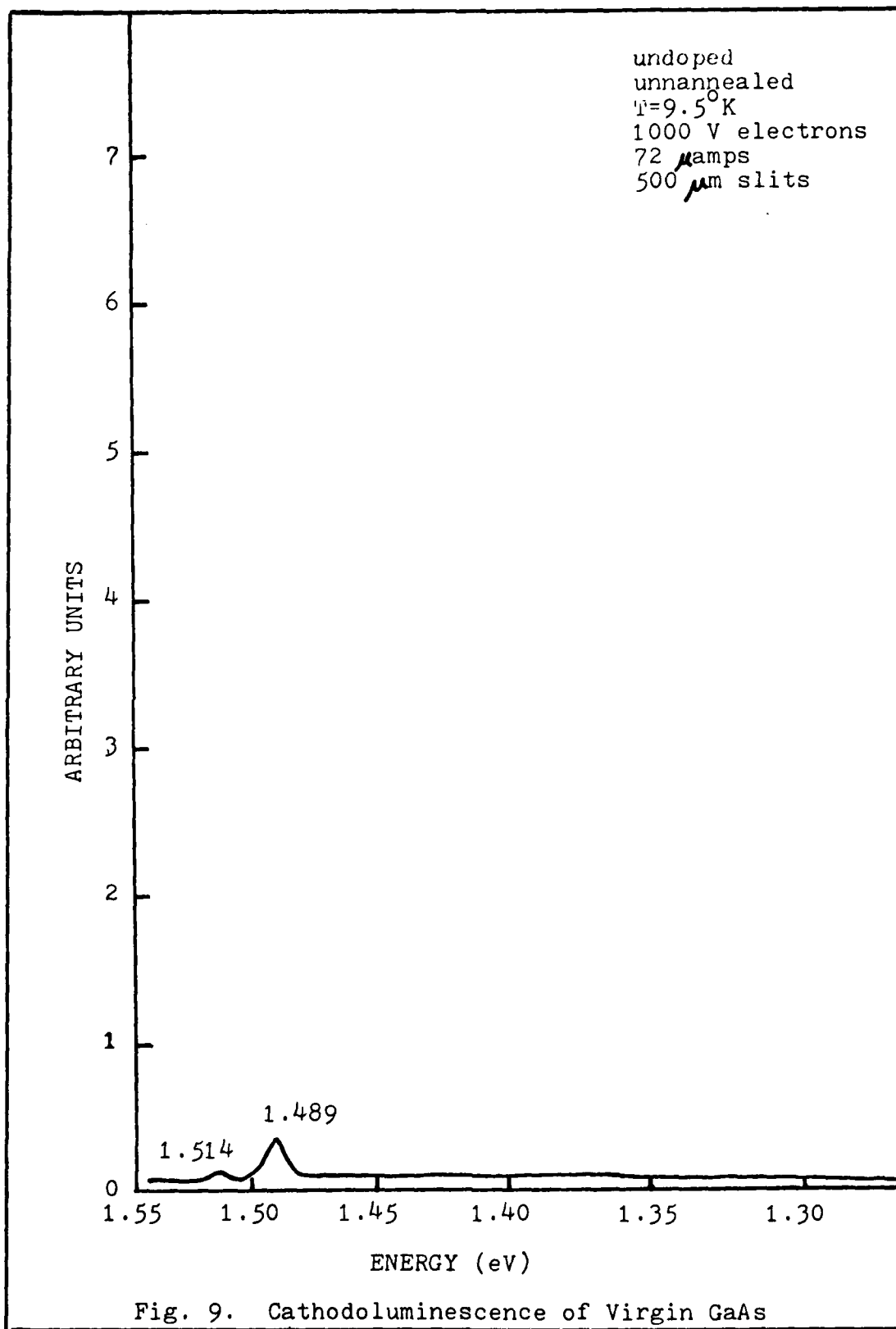


Fig. 9. Cathodoluminescence of Virgin GaAs

in this study: sample 4 at 800°C for 10 minutes, sample 5 at 800°C for 10 seconds, sample 10 at 900°C for 10 minutes, and sample 11 at 900°C for 10 seconds.

Sample 4, Figure 10, exhibited a peak at 1.515 eV \pm 0.009 associated with a free exciton annihilation and a peak at 1.491 eV \pm 0.009 associated with a free electron-bound hole recombination. Also seen were peaks at 1.451 eV, 1.361 eV, and 1.326 eV. The peak at 1.451 eV is assumed to be a phonon replica of the 1.491 eV peak since it is approximately 36 meV from the 1.491 eV peak and there were no other impurities found in the crystal which could account for the peak. The 1.361 eV peak is assumed to be a vacancy complex, possibly a $V_{As}-Si_{As}$ complex (Ref. 5:622). The peak at 1.326 eV appears to be a phonon replica of the peak at 1.361 eV. The 1.491 eV peak dominates all the spectra taken from this sample, but appears greatest near the surface and decreases as do the other peaks, as the crystal is etched deeper.

Sample 5, Figure 11, exhibits a line at 1.515 eV \pm 0.009 associated with a free exciton annihilation, and a peak at 1.489 eV \pm 0.009 associated with a free electron-bound hole recombination. After etching in 250 Å a peak at 1.459 eV and a peak at 1.359 eV appeared. The 1.459 eV peak may be the Q band referred to by Swaminathan (Ref. 34:155). The peak at 1.359 eV appears to be the same as the one seen in sample 4, a vacancy complex. The 1.489 eV peak is dominant in all the spectra taken from this sample. The intensities of the spectra in general appear to be greatest after a 250 Å etch

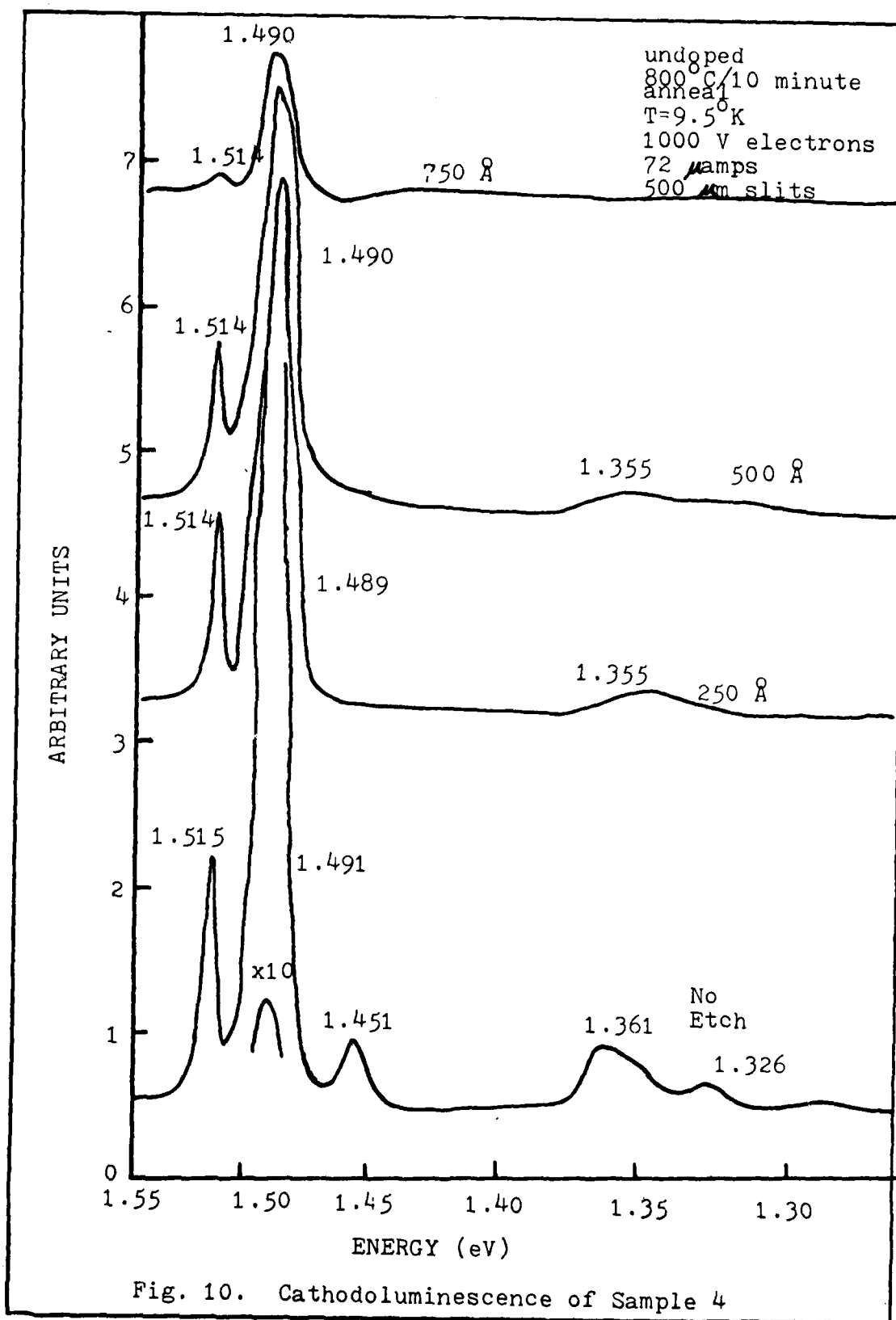


Fig. 10. Cathodoluminescence of Sample 4

then decline as the material is etched deeper. It appears that the major effects of the 300°C/10 second anneal were maximized between 250 and 500 Å into the crystal.

Sample 10, Figure 12, exhibits one large peak that starts at 1.429 eV \pm 0.009 at the surface of the crystal, but migrates to 1.448 eV as the sample was etched to 750 Å. The peak exhibited a small shoulder at about 1.483 to 1.488 eV. The shoulder appears to be the free electron-bound hole recombination observed in other samples. After etching in 250 Å the sample showed a weak line at 1.513 eV associated with a bound exciton annihilation, but this line disappeared after an additional etch. The shifting of the 1.429 eV peak is similar to the behavior observed by Pomrenke (Ref. 31).

Sample 11, Figure 13, initially showed only a small Bound exciton annihilation peak at 1.513 eV \pm 0.009 and a free electron-bound hole recombination peak at 1.489 eV \pm 0.009. The exciton peak was initially larger than the free electron-bound hole peak unlike the other samples, and the spectrum was very weak. After etching in 500 Å the 1.489 eV peak is now dominant in the spectrum and the intensity of the spectrum is now much stronger. The 1.489 eV peak now exhibits a shoulder at 1.485 eV and a phonon replica at 1.453 eV. The 1.485 eV peak is possibly a free electron-bound hole or a bound electron-bound hole recombination involving Si. After etching in 750 Å the spectrum remains the same but is decreased in intensity indicating that the effects

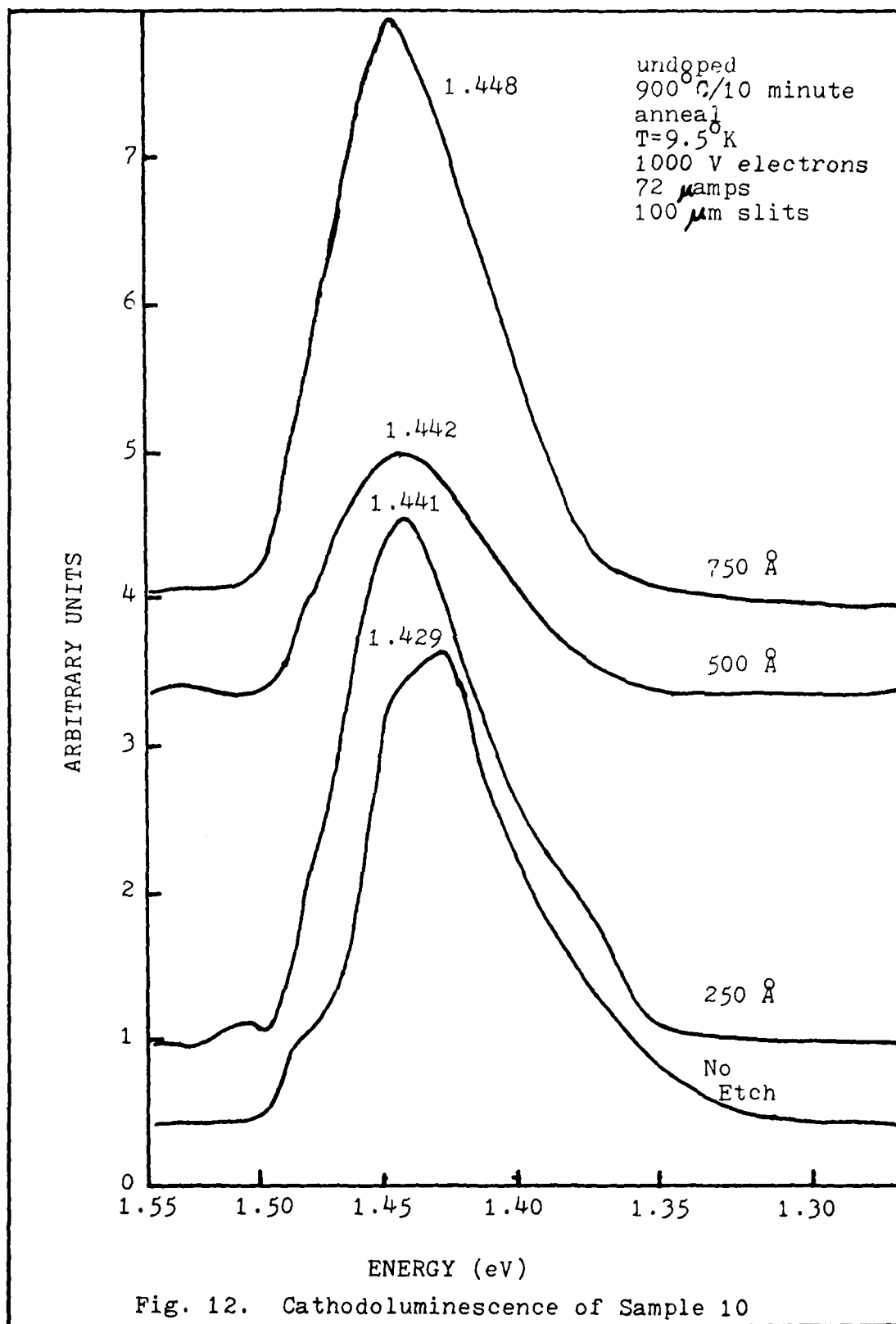


Fig. 12. Cathodoluminescence of Sample 10

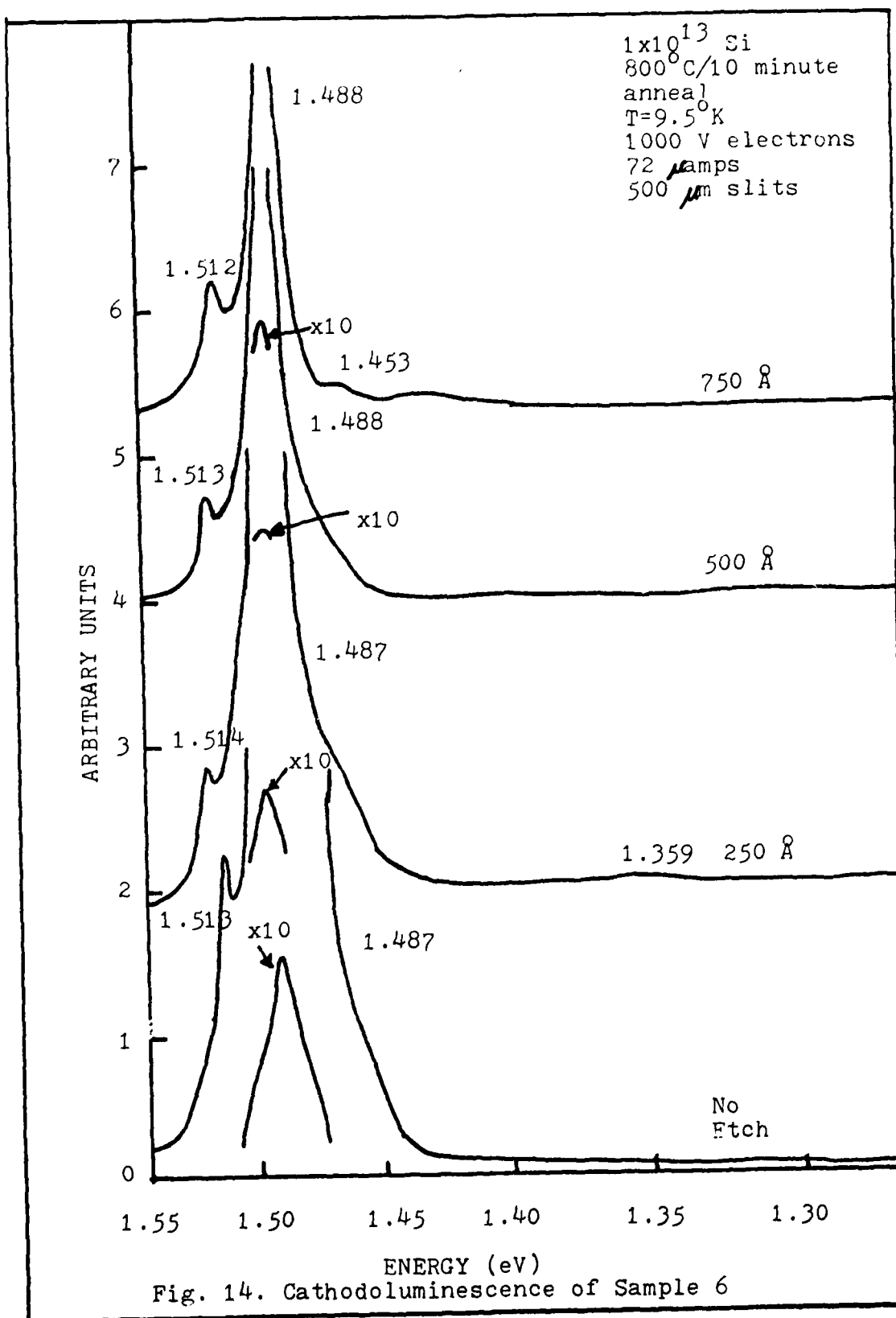
of the 900°C/ 10 second anneal are maximized between 500 and 750 Å into the crystal.

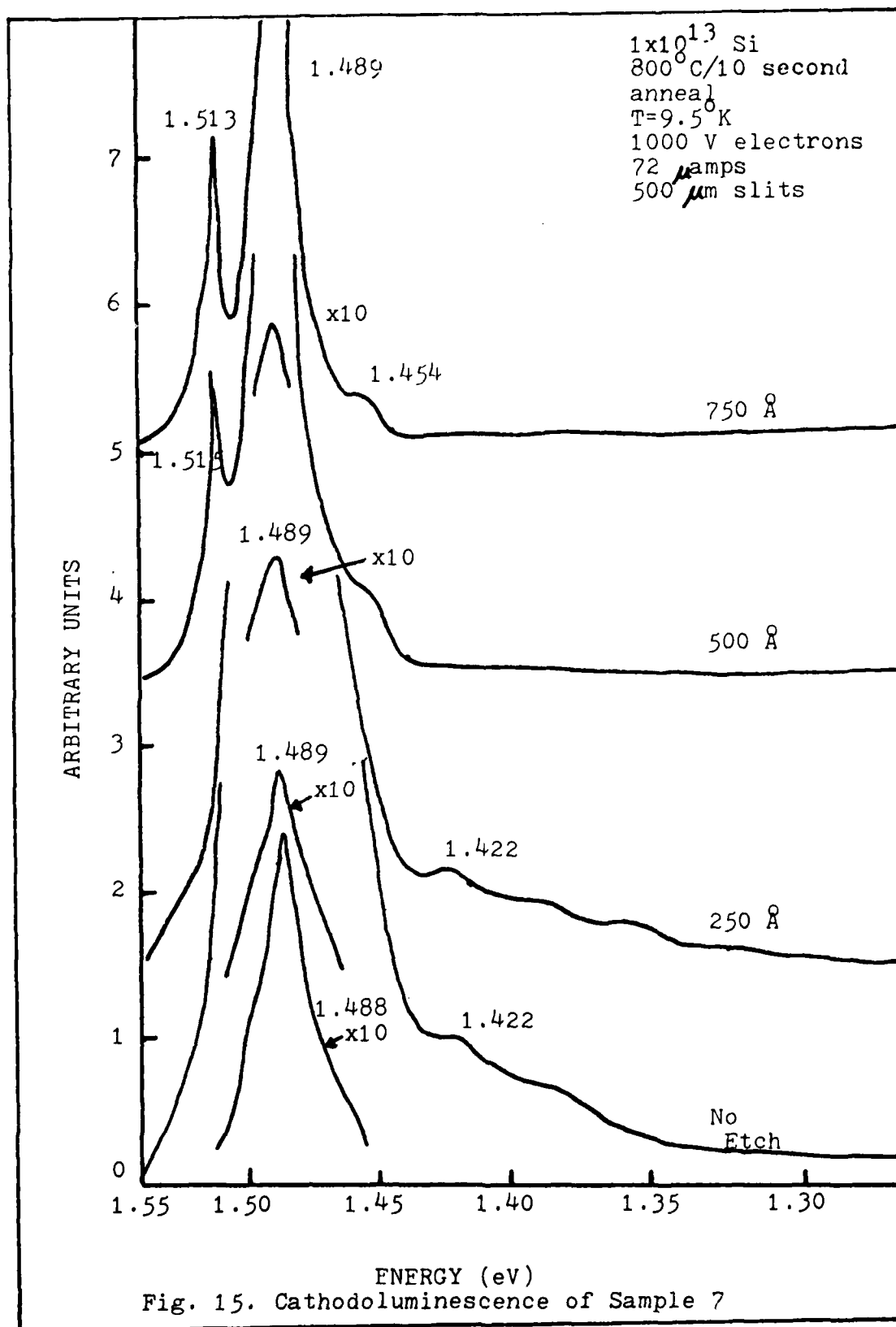
Annealed Si Implanted GaAs

Four samples of GaAs were implanted with 100 keV Si at a fluence of 10^{13} cm⁻² and annealed for the same temperatures and times as the unimplanted samples: sample 6 at 800°C for 10 minutes, sample 7 at 800°C for 10 seconds, sample 12 at 900°C for 10 minutes, and sample 13 at 900°C for 10 seconds.

Sample 6, Figure 14, exhibited a bound exciton peak at 1.513 eV \pm 0.009, a strong free electron-bound hole recombination at 1.487 eV \pm 0.009, and a weak vacancy complex peak at 1.359 eV \pm 0.009. The 1.487 eV peak was much stronger than it was in the unimplanted samples. The intensity of the spectra decreased as the material was etched away. After etching in 250 Å a shoulder appeared on the 1.487 eV peak which resolved into a phonon replica after an etch of 750 Å. The 1.487 eV peak migrated to 1.488 eV after etching 500 Å into the crystal.

Sample 7, Figure 15, initially exhibited a very strong peak at 1.489 eV. The peak overshadowed the region in which the exciton peak normally existed in this spectrum. Two shoulders on the peak were prominent at 1.422 eV and 1.391 eV. The peak at 1.422 eV appears to be the Q band and the 1.391 eV peak appears to be a phonon replica of the 1.422 eV peak. As the crystal is etched deeper the 1.489 eV peak decreases. After etching in 500 Å the free exciton peak at 1.515 eV





appears and the Q band has disappeared. A shoulder appears on the 1.489 eV peak at 1.454 eV which is probably a phonon replica of the 1.489 eV peak. After etching in 750 Å the 1.454 eV peak has become fully resolved.

Sample 12, Figure 16, initially exhibits a peak at 1.465 eV with a shoulder at 1.482 eV. The 1.465 eV peak is probably the Q band seen in the unimplanted 900°C/10 minute annealed sample. The shoulder is probably the free electron-bound hole recombination seen in the other samples. The luminescence from this sample was so intense that it was necessary to close the spectrometer slits from 500 m to 100 m. After etching in 250 Å the peak shifted to 1.468 eV and the leading edge of the peak (that part associated with higher energy photons) became very sharp. The free electron-bound hole peak may now be very strong causing this sharp leading edge, and is combining with the Q band peak to create one large peak. This appears to be the case, after etching in 750 Å. The peak is now located at 1.484 eV and has a very long tail on the trailing edge of the peak indicating that the Q band is still there but diminished. The exciton peak at 1.515 eV appears after etching 250 Å into the crystal.

Sample 13, Figure 17, initially exhibited a peak at 1.471 eV and a bound exciton peak at 1.514 eV. The 1.471 eV peak appears to be a combination of the free electron-bound hole peak and the Q band again. After etching in 250 Å a shoulder appears at 1.481 eV. After etching in 500 Å the

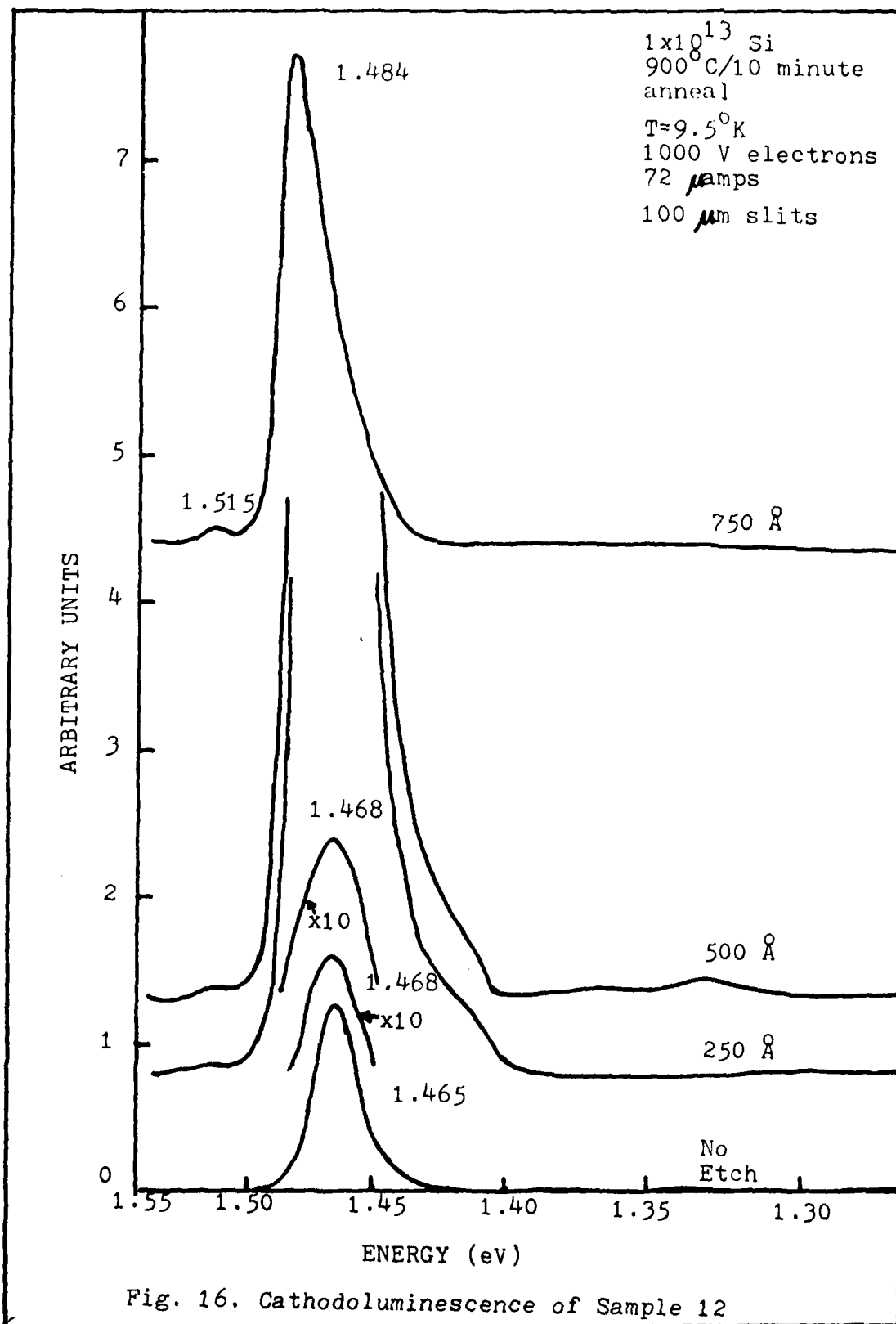
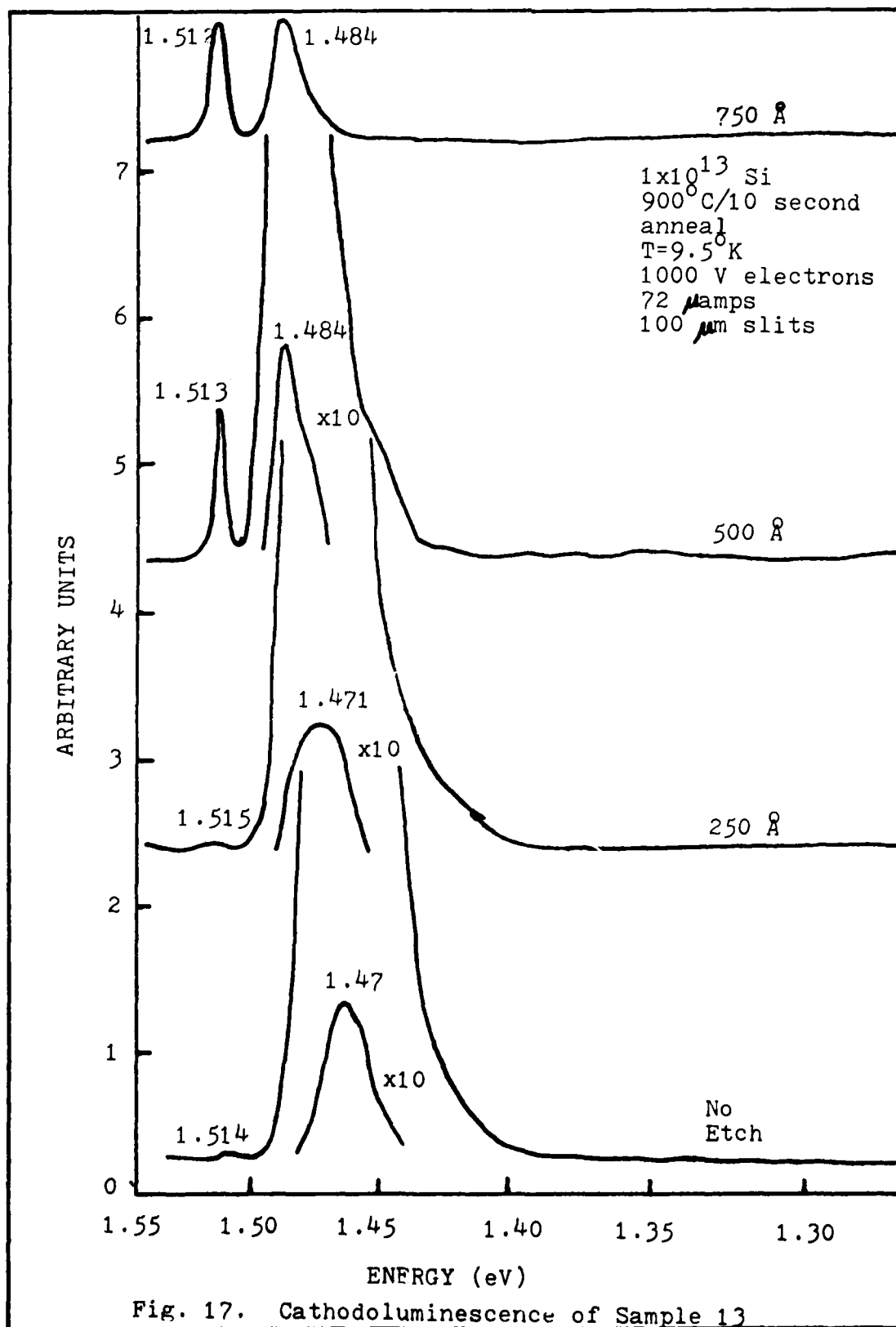


Fig. 16. Cathodoluminescence of Sample 12



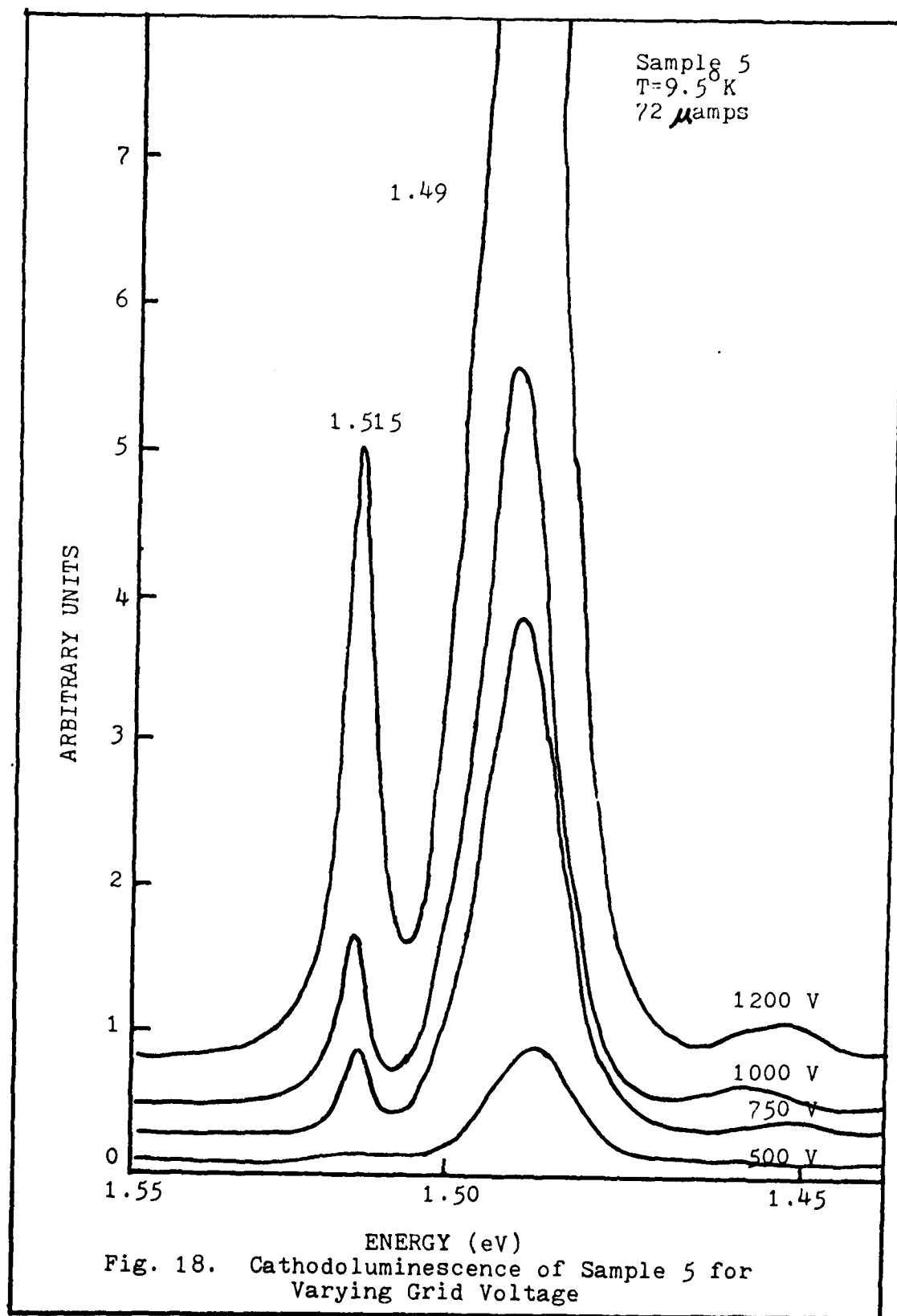
peak has shifted to 1.484 eV and the Q band now shows up as a shoulder on the 1.484 eV peak. The 1.513 eV peak has increased in size now, and so has the 1.484 eV peak. After etching in 750 Å the Q band has now disappeared and the exciton peak and the free electron-bound hole recombination peak are decreasing. The effects of the annealing in this case appear to be maximized between 500 and 750 Å into the crystal.

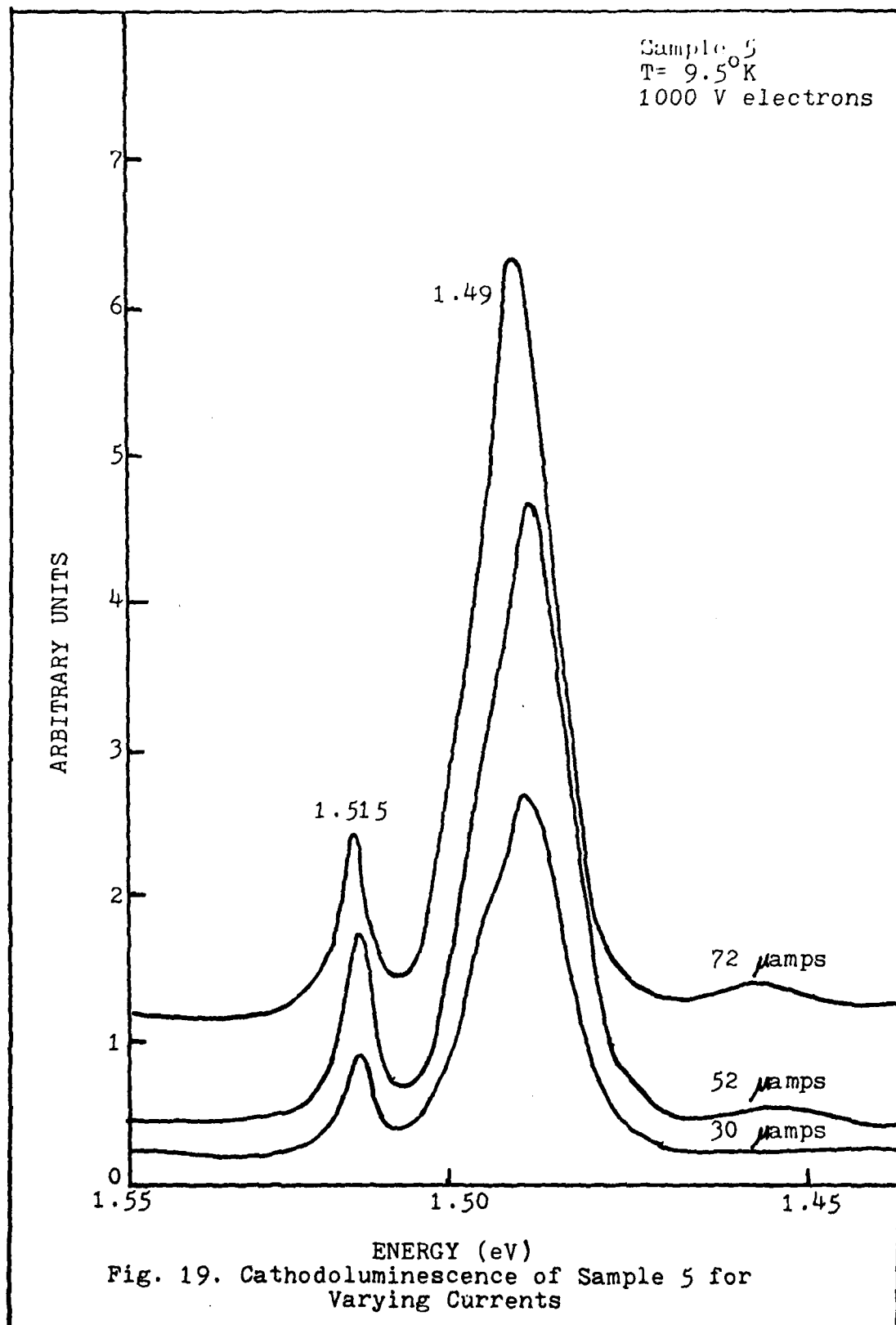
Effects of Electron Gun Voltage and Current on the Cathodoluminescence Spectra

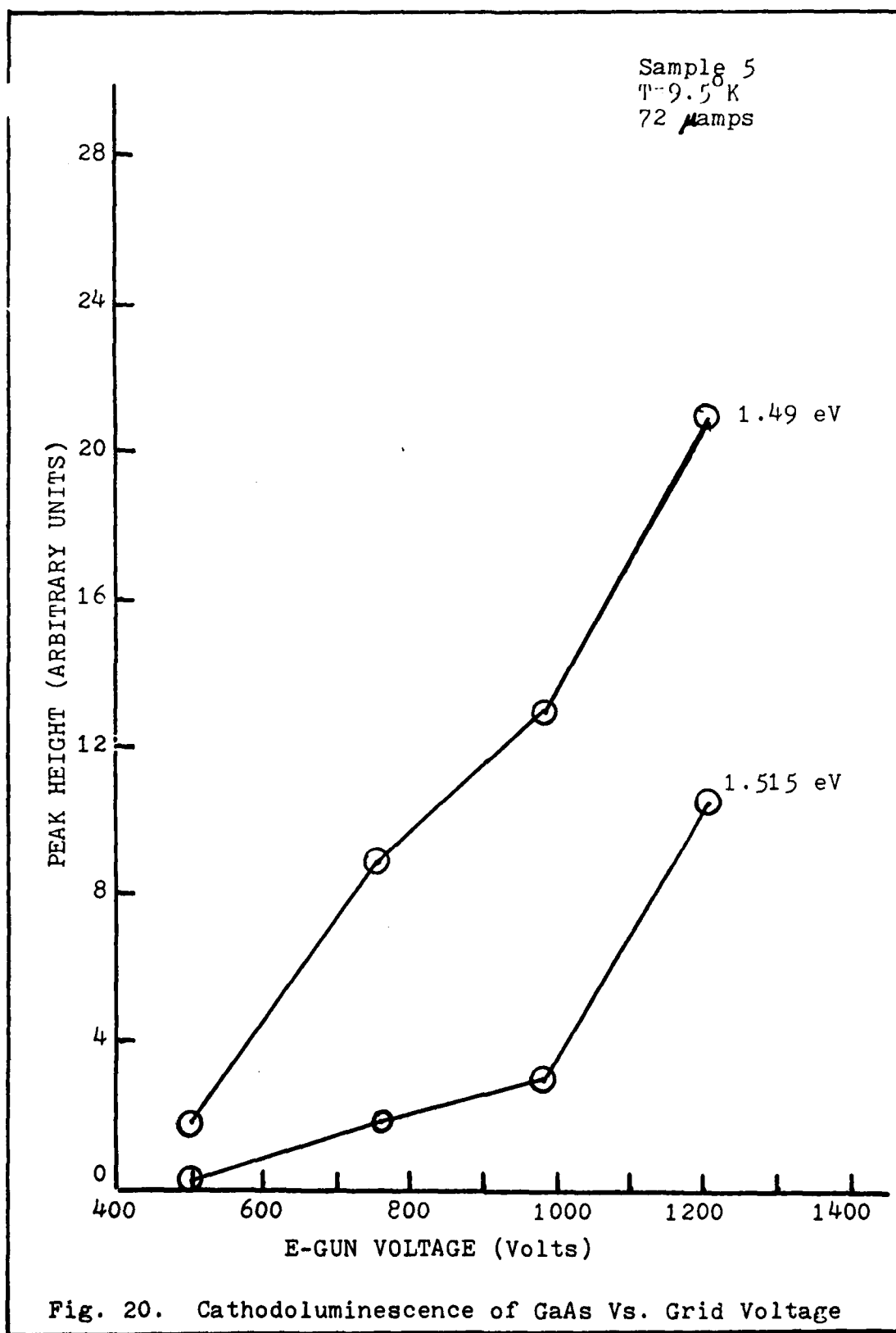
Spectra were taken on sample 5 before etching, varying the electron gun current and grid voltage. These measurements were taken to determine the effects of fluctuations in gun voltage and current on the luminescence data. The results are shown in Figures 18, 19, 20, and 21. The effects on the spectra of increasing the electron gun current indicated that the intensity of the spectra would reach a plateau. This would be consistent with saturating the region of excitation. It can be seen from Figure 21 that small fluctuations in current will have only a minor effect on the luminescence data. Increases in grid voltage, Fig. 20, cause large changes in the luminescence. Fortunately grid voltage was controllable to ± 1 V.

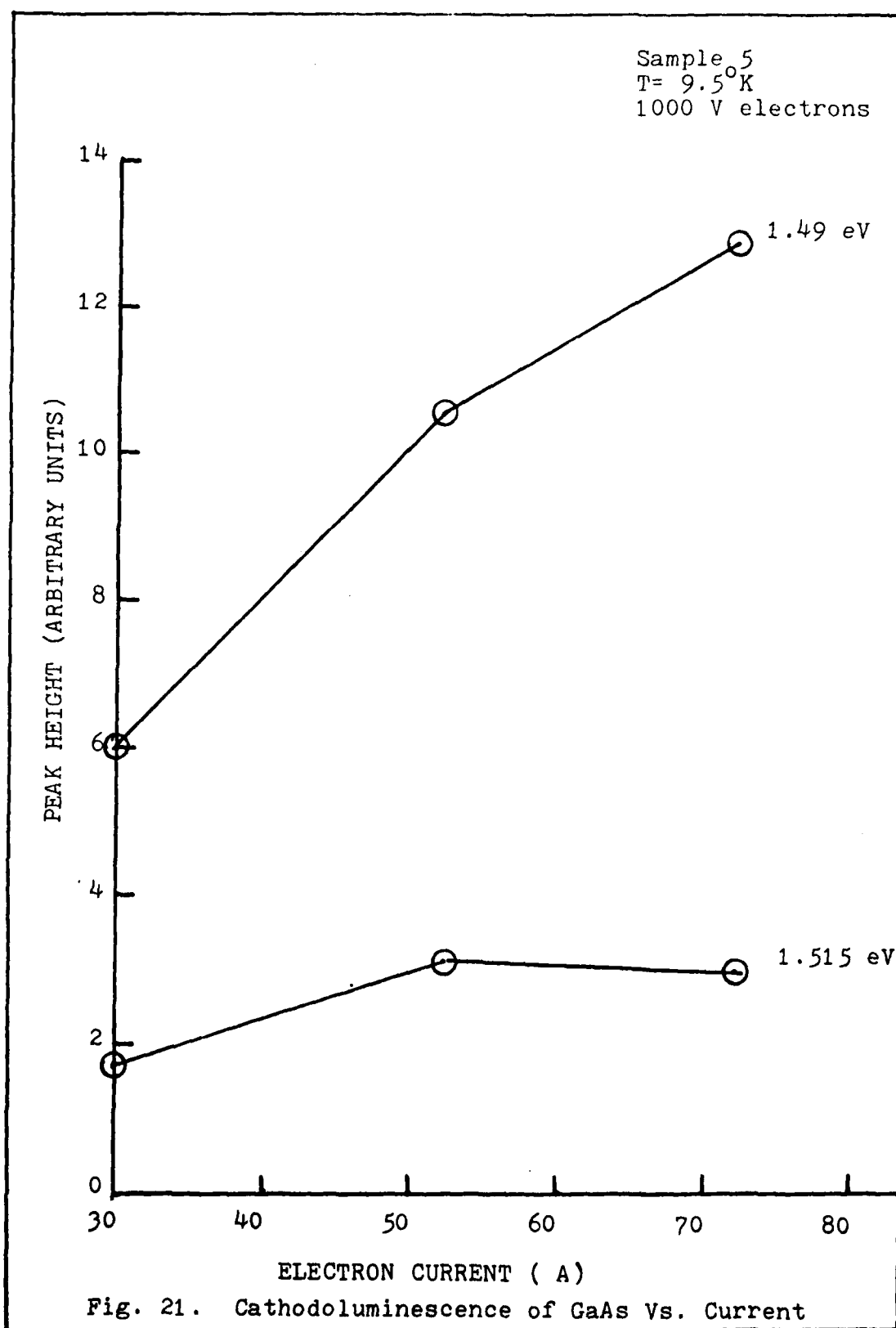
Discussion

The virgin GaAs exhibits very little luminescence. Apparently there are non-radiative processes occurring









in the virgin material. Whether this is due to the manufacturer's growth technique, the chemo-mechanical polishing, or some other process used on the crystal is unknown. It can be seen though that annealing the virgin material can significantly increase the radiative processes in the crystal. It appears that the 800°C/10 minute anneal was most effective on optically activating the virgin material, followed by the 800°C/10 second anneal. The 900°C/10 minute anneal produced a large vacancy complex peak in the material which dominated the spectrum, and the 900°C/10 second anneal still possessed non-radiative processes near the surface (0 to 250 Å) but showed positive effects from the annealing after the 500 Å etch.

The free electron-bound hole recombination in all the spectra is assumed to be a Si acceptor since the spark source mass spectroscopic analysis did not show any other impurity with a recombination energy near the 1.490 eV peak of Si. All recombinations identified as free electron-bound hole recombinations were approximately the energy of the conduction band to Si acceptor recombination to within the accuracy of the measurement.

The implanted samples all showed a much more intense spectra in general than the unimplanted samples. However, sample 12 showed a considerably reduced luminescence in the first 250 Å of the material indicating non-radiative processes were occurring.

The 900°C annealed implanted samples show a much

greater optical activation of the implant and the native crystal than the 800°C annealed samples. They also show an increase in the number of vacancy complexes generated as evidenced by the shifts of the peaks to lower energies near the surface of the crystals. The 900°C/10 second anneal (sample 13) showed advantages over the 900°C/10 minute anneal (sample 12) in that the shift to lower energies was much less (1.47 eV versus 1.465 eV) and the 1.484 eV Si acceptor peak returned to dominate the spectrum after only a 500 Å etch versus the 750 Å etch required for sample 12.

Sample 7 appeared to have a greater luminescence than sample 6 indicating an advantage of the 10 second anneal over the 10 minute anneal. However, sample 7 also showed evidence of vacancy complexes in the surface of the material (peaks at 1.422 eV and 1.391 eV).

In the unimplanted samples the 800°C/10 minute anneal (sample 4) appeared to be the most effective. Sample 4 had the greatest luminescence of all the unimplanted samples except sample 10. Sample 10 had only a large vacancy peak for luminescence. Samples 5 and 11, the 10 second anneals both had lower intensity spectra near the surface indicating that some non-radiative processes were still occurring.

The numbers representing the etch depths for all samples are estimates. The etch solution was calibrated using a very long etch (2 hours) then measuring the etch depth using the Sloan Dektak Surface Profile Machine. This gave

an average etch rate of $36.14 \text{ \AA}/\text{minute}$. When the samples were measured on the Dektak it exhibited instabilities characterized by an inability to level the sample and a drifting of the stylus. This may have been a result of having to use a more sensitive scale to measure the smaller etch depth.

V Conclusions and Recommendations

Conclusions

The effects of long time (10 minute) and short time (10 second) annealing on GaAs were studied and the following conclusions were reached:

- 1) Annealing of the samples used in this study caused an increase in the luminescence for both implanted and unimplanted samples. This indicates that there are either non-radiative processes present in the virgin GaAs:Cr or that impurities are entering the samples during the annealing process.
- 2) Non-radiative processes were still present in the surface of the 10 second annealed samples, but optical activation was occurring deeper into the crystal.
- 3) The 800°C/10 minute anneal was most effective in optically activating the impurities in the unimplanted samples.
- 4) The 900°C/10 second anneal was most effective in optically activating the impurities in the implanted samples.
- 5) The 900°C/10 minute anneal created excessive vacancy complexes in the crystal.

The short time anneal showed definite promise for optically activating implants in GaAs. However additional studies need

to be done.

Recommendations

The following recommendations are made for future studies on annealing GaAs:

- 1) Perform depth-resolved luminescence at temperatures higher than 900°C for short times and etch deeper into the crystal.
- 2) Extend short annealing times to 20 and 30 seconds.
- 3) Perform short time annealing on samples implanted with fluences of 10^{14} and 10^{15} cm^{-2} .
- 4) Link the cathodoluminescence data to data taken on depth-resolved electrical properties of the samples.
- 5) Measure the thickness of the damage layer created chemo-mechanical polishing of crystals.

Bibliography

1. Air Force Avionics Laboratory. Technical Programs and Contracts (Tenth Edition). March 1979.
2. Aoki, K., et al. "Depth Distribution of Defects in Mg-Ion and Cd-Ion Implanted GaAs," Japanese Journal of Applied Physics, 15(2):405-406 (February 1976).
3. Ashen D. J., et al. "The Incorporation and Characterization of Acceptors in Epitaxial GaAs," Journal of Physics and Chemistry of Solids, 36(10):1041-1053 (October 1975).
4. Bebb, H. B., et al. "Photoluminescence I: Theory," Semiconductors and Semimetals, Volume 8, edited by R. W. Willardson and Albert C. Beer. New York: Academic Press, 1972.
5. Birey, H. and J. Sites. "Radiative Transitions Induced in Gallium Arsenide by Modest Heat Treatment," Journal of Applied Physics, 51(1):619-624 (January 1980).
6. Bogardus E. H. and H. B. Bebb. "Bound-Exciton, Free-Exciton, Band Acceptor, Donor Acceptor, and Auger Recombination in GaAs," Physical Review, 176(3):993-1002 (December 1968).
7. Boulet, D. L. Depth Resolved Cathodoluminescence of Cadmium Implanted Gallium Arsenide. Unpublished MS thesis. Wright-Patterson Air Force Base, Ohio: Air Force Institute of Technology, December 1975.
8. Chatterjee, P. K., et al. "Photoluminescence from Be-Implanted GaAs," Applied Physics Letters, 27(10):567-569 (November 1975).
9. Chatterjee, P. K., et al. "Photoluminescence Study of Native Defects in Annealed GaAs," Solid State Communications, 17:1421-1424 (1975).
10. Colbaw, K. "Free-to-Bound and Bound-to-Bound Transitions in CdS," Physical Review, 141(2):742-749 (January 1966).
11. Cusano, D. A. "Identification of Laser Transitions in Electron-Beam Pumped GaAs," Applied Physics Letters, 7(6):151-152 (September 1965).
12. DeForest, D. L., Cathodoluminescence and Photoluminescence of Silicon Implanted Gallium Arsenide, Unpublished MS thesis. Wright-Patterson Air Force Base, Ohio: Air Force Institute of Technology, March 1982.

13. Dmitruk, N. L., et al. "Electrophysical and Luminescence Properties of Implanted GaAs," Radiation Effects, 49:51-56 (1980).
14. Feldman, Charles. "Range of 1-10keV Electrons in Solids," Physical Review, 117(2):455-459 (January 1960).
15. Gavrilov, A., et al. "Photoluminescence Investigation of the Distribution of Defects in Gallium Arsenide After Ion Bombardment," Soviet Physics of Semiconductors, 10(8):847-848 (August 1976).
16. Gershenzon, M. "Radiative Recombination in III-V Compounds," Semiconductors and Semimetals, Volume 2, edited by R. K. Willardson and Albert C. Beer. New York: Academic Press, 1966.
17. Gibbons, James F. "Ion Implantation in Semiconductors-Part I: Range Distribution Theory and Experiments," Proceedings of the IEEE, 56(3):295-319 (March 1968).
18. Gibbons, James F. Projected Range Statistics. Stroudsburg, Pa: Dowden, Hutchinson and Rose, Inc., 1975.
19. Iida, Shinya and Kazuhiro Ito. "Selective Etching of Gallium Arsenide Crystals in $H_2SO_4-H_2O_2-H_2O$ System," Journal of the Electrochemical Society: Solid State Science, 118(5):768 (May 1971).
20. Key, M. V. Photoluminescence Study of Ion Implantation Damage in Gallium Arsenide. Unpublished MS thesis. Wright-Patterson Air Force Base, Ohio: Air Force Institute of Technology, December 1981.
21. Kittel, C. Introduction to Solid State Physics. New York: John Wiley and Sons, 1971.
22. Kolthoff, K. M., et al. Volumetric Analysis, Volume 3. New York: Interscience Publishers, Inc., 1957.
23. Lindhard, J., et al. "Range Concepts and Heavy Ion Ranges," Mat. Fys. Medd. Dan. Vid., Selsk 33:1 (1963).
24. Maclin, M. T. Depth Resolved Luminescence of Gallium Arsenide using Ion Etching. Unpublished MS thesis. Wright-Patterson Air Force Base, Ohio: Air Force Institute of Technology, December 1981.
25. Martinelli, R. U. and C. C. Wang. "Electron-Beam Penetration in GaAs," Journal of Applied Physics, 44(7):3350-3351 (July 1975).

26. McKelvey, J. P. Solid State and Semiconductor Physics. New York: Harper and Row, 1966.
27. Morgan, D. V. "The Characterization and Application of Ion-Induced Damage in Gallium Arsenide Devices," Radiation Physics and Chemistry, 15(5):627-636 (March 1980).
28. Norris, C. B. and C. E. Barnes. "Cathodoluminescence Studies of Anomalous Ion Implantation Defect Introduction in Lightly and Heavily Doped Liquid Phase Epitaxial GaAs:Sn," Journal of Applied Physics, 51(11):5764-5772 (November 1980).
29. Pankove, Jacques I. Optical Processes in Semiconductors. Englewood Cliffs, NJ:Prentice Hall, Inc., 1971.
30. Pierce, B. J. Luminescence and Hall Effects of Ion Implanted Layers of ZnO. Unpublished dissertation. Wright-Patterson Air Force Base, Ohio: Air Force Institute of Technology, September 1974.
31. Pomrenke, G. S., et al. "Luminescence Characteristics of the 1.4 eV Silicon Related Complex in GaAs," Unpublished paper. Wright-Patterson Air Force Base, Ohio: AFWAL/AADR
32. Seki, Y., et al. "Properties of Epitaxial GaAs Layers from a Triethyl Gallium and Arsine System," Journal of Electrochemical Society: Solid State Science and Technology, 122(8):1108-1112.
33. Sturge, M. D. "Optical Absorption of Gallium Arsenide Between 0.6 and 2.75 eV," Physical Review, 127(3):768-773 (August 1962).
34. Swaminathan V., et al. "Photoluminescence of Thermally Treated n Si-Doped and Semi-Insulating Cr-Doped GaAs Substrates," Journal of Luminescence, 22:153-170 (1981).
35. Williams, E. W. and C. T. Elliott. "Luminescence Studies of a New Line Associated with Germanium in GaAs," British Journal of Applied Physics, 2(2):1657-1665 (February 1969).
36. Williams, E. W., et al. "Photoluminescence II: Gallium Arsenide," Semiconductors and Semimetals, Volume 8, edited by R. K. Willardson and Albert C. Beer. New York: Academic Press, 1972.

Vita

Jeffrey Ray Cavins was born August 15, 1957 in Weibaden AFB, Germany. He spent his childhood years in Belleville, Illinois, Memphis, Tennessee, Birmingham, Alabama, and finally Orlando, Florida. He attended Edgewater High School in Orlando where he was a member of the National Honor Society and the Russian Club. He graduated from high school in June 1975 and entered Florida Technological University in September 1975. In the summer of 1976 he entered the AFROTC program and was granted a 2year ROTC scholarship. He graduated with a B. S. in physics from FTU in June 1978. In October 1978 he was called to active duty and assigned to the Air Force Weapons Laboratory, Pulsed Laser Systems Branch, Kirtland AFB, New Mexico, where he became Chief Scientist for the Pulsar Laser Project. In June 1978 he was reassigned to the Air Force Institute of Technology where he pursued a Master of Science degree in Engineering Physics.

REPORT DOCUMENTATION PAGE		READ INSTRUCTIONS BEFORE COMPLETING FORM
1. REPORT NUMBER	2. GOVT ACCESSION NO.	3. PERFORMING ORG. REPORT NUMBER
	AD-A124705	
4. TITLE (and Subtitle)	5. TYPE OF REPORT & PERIOD COVERED	
DEPTH-RESOLVED CATHODOLUMINESCENCE STUDY OF ANNEALED SILICON IMPLANTED GALLIUM ARSENIDE		
7. AUTHOR(s)	6. PERFORMING ORG. REPORT NUMBER	
Jeffrey R. Cavins Air Force Institute of Technology		
9. PERFORMING ORGANIZATION NAME AND ADDRESS	8. CONTRACT OR GRANT NUMBER(s)	
Air Force Institute of Technology (AFIT/ENA) Wright-Patterson AFB, Ohio 45433		
11. CONTROLLING OFFICE NAME AND ADDRESS	10. PROGRAM ELEMENT, PROJECT, TASK AREA & WORK UNIT NUMBERS	
AFIT/ENA		
14. MONITORING AGENCY NAME & ADDRESS (if different from Controlling Office)	12. REPORT DATE	
	December 1982	
	13. NUMBER OF PAGES	
	72	
	15. SECURITY CLASS. (of this report)	
	Unclassified	
	15a. DECLASSIFICATION/DOWNGRADING SCHEDULE	
16. DISTRIBUTION STATEMENT (of this Report)		
Approved for public release; distribution unlimited.		
17. DISTRIBUTION STATEMENT (of the abstract entered in Block 20, if different from Report)		
18. SUPPLEMENTARY NOTES		
<p>Approved for public release; LAW AFR 190-17.</p> <p><i>John E. Wolaver</i> JOHN E. WOLAVER Dean for Research and Professional Development Air Force Institute of Technology (AFIT) Wright-Patterson AFB OH 45433</p> <p>19 JAN 1983</p>		
19. KEY WORDS (Continue on reverse side if necessary and identify by block number)		
Gallium arsenide; Depth profile; Annealing; Ion implantation; Silicon implant		
20. ABSTRACT (Continue on reverse side if necessary and identify by block number)		
<p>Depth-resolved cathodoluminescence was performed on Si ion implanted GaAs. Nine samples were prepared for this study, four were implanted with 100 keV Si ions at a fluence of 10^{13} atoms/cm², and five were left unimplanted. One each of the implanted and the unimplanted samples were annealed at 800°C for 10 minutes, 800°C for 10 seconds, 900°C for 10 minutes, or 900°C for 10 seconds, for a total of eight</p>		

C

samples. The ninth sample was left unimplanted and unannealed as a control. Cathodoluminescence data was taken using 1000 V electrons as an excitation source. Depth resolution was achieved by taking spectral data and successively chemically etching the surface of the crystal in 250 Å steps.

No new peaks were observed in the GaAs during the experiment. Data indicated that the 900°C/10 second anneal was superior in optically activating the impurities in the implanted samples. The 800°C/10 minute anneal proved to have the greatest effect in optically activating the impurities in the unimplanted samples. The 900°C/10 minute anneals exhibited spectra associated with vacancy complexes. It should be noted that the virgin GaAs control sample exhibited evidence that non-radiative processes were occurring, suppressing the spectra from the sample.

K